

Megabenthic Biotope Composition of the Rockall
Escarpment, Northeast Atlantic

By Ashley Nickson

A thesis submitted to the Department of Ocean Sciences in partial fulfillment of the
requirements for a Bachelor of Science degree with Honours in Marine Biology

March 27th, 2023

Abstract

The depths of the ocean have been largely shrouded in the unknown. However, technological advances made in the past 60 years have provided researchers with the opportunity to start unravelling the complexities of the deep sea. There is now an understanding that the deep sea is host to a complex and diverse mosaic of communities that we also realize are in peril due to the effects of climate change.

This thesis examined the biodiversity patterns and biotope composition present within the Rockall Escarpment, situated in the Northeast Atlantic Ocean. We used data that was annotated from images across nine transects, totalling to 16,150 m, obtained by a Remotely Operated Vehicle. Benthic community composition was assessed across the whole study area using Non-Metric Multidimensional Scaling (nMDS), followed by SIMPER, and indicator species analysis to classify the benthic taxa observed into biotopes. In total, 59,418 individual organisms representing 199 megafaunal morphospecies were analyzed. Twelve biotopes were identified, biotopes five, six, nine, and twelve composed of vulnerable sessile taxa including the cold-water corals *Solenosmilia variabilis*, *Madrepora oculata*, and *Desmophyllum pertusum*.

Substrate, food availability and currents are among the most significant factors influencing the complex geomorphology and consequently, the distribution of megafaunal species. Determining the megafaunal species richness and abundance present, and the factors that affect their distribution, provide insights into vulnerable biotopes. Understanding the vulnerable biotopes present will ultimately contribute to our

baseline knowledge of the distribution of taxa in the Northeast Atlantic and hopefully, management measures that are climate adaptive.

Acknowledgements

This project was made possible with the help and support of many people.

I would like to thank my supervisor, Dr. Katleen Robert of the Fisheries and Marine Institute of Memorial University of Newfoundland and Labrador, whose passion for student growth and development was instrumental to my success.

I would also like to express my deepest gratitude to my mentor Emmeline Broad who was always there to lend a helping hand. She believed in me from the start and invested personal time and effort in helping other women succeed.

I would like to extend a big thank you to the 4D Oceans lab for their invaluable guidance and shared experiences.

Lastly, I would like to thank the Irish Marine Institute through the Marine Research Sub-Programme of the Irish Government, for which the data for this research was acquired during the CE14011 SORBEH expedition.

Author Contributions

Dr. Katleen Robert was responsible for the data collection, identification, and annotation of species in ROV imagery.

Emmeline Broad supervised Ashley Nickson in compiling the statistical coding in R.

Ashley Nickson conducted the statistical analysis and all writing of the honour's dissertation with inputs from Emmeline Broad and Dr. Katleen Robert.

Table of Contents

<i>Abstract</i>	<i>ii</i>
<i>Acknowledgements</i>	<i>iv</i>
<i>Author Contributions</i>	<i>v</i>
<i>Table of Contents</i>	<i>vi</i>
<i>List of Tables</i>	<i>vii</i>
<i>List of Figures</i>	<i>viii</i>
<i>List of Abbreviations</i>	<i>x</i>
<i>List of Appendices</i>	<i>xi</i>
1. Introduction	1
2. Methods	5
2.1 Study Area	5
2.2 Data Collection	7
2.3 Statistical Analysis	11
3. Results	13
3.1 Megafaunal community structure	13
3.2 Biotope description	20
4. Discussion	27
4.1 Conservation	30
4.2 Importance of a biotope under climate change	31
5. Conclusion	32
6. References	32
7. Appendices	48
7.1 Species ID for all discriminating species assigned from SIMPER and IndVal	48
7.2 Results from the SIMPER analysis per biotope with the cumulative summary representing approximately 75% of the dissimilarity between the biotope pairs	51
7.3 Results from indVal analysis per biotope indicating the most representative species in each community	62
7.4 Fusion levels from the dendrogram of \log_{x+1} and Hellinger with Bray-Curtis UPGMA clustering	68

List of Tables

Table 1. Summary of ROV dives and video transects assessed.

Table 2. Biotope summary table with discriminating species resulting from both SIMPER and IndVal.

List of Figures

Figure 1. Bathymetry map of the full study site with the locations of the nine ROV dive sites across the Rockall escarpment. Map projection is UTM zone 28N.

Figure 2. UPGMA hierarchical clustering dendrogram by Hellinger and Bray-Curtis dissimilarity matrix depicting the resultant 12 coloured biotope clusters.

Figure 3. Images of the discriminating morphospecies for each biotope: a. Anthozoa species 1, b. Holothuroidea species 4, c. Echinoidea species 2, d. Anthozoa species 14, e. Leiopathes species, f. Demospongiae, g. Ophiuroidea species 1, h. Echinoidea species 1, i. Anthozoa species 8, j. *Parastichopus* species, k. *Asconema foliatum*, l. Phakellia, m. Flabellidae, n. Demospongiae, o. *Desmophyllum pertusum*, p. Reteporella, q. Porifera species 6, r. Porifera species 3, s. Ascidiacea, t. Anthozoa species 6, u. Ophiuroidea species 2, v. *Madrepora oculata*, w. *Araesoma fenestratum*, x. *Cidaris cidaris*, y. Ophiuroidea species 4, z. Anthozoa species 5 and 1. Crinoidea species 2.

Figure 4. Species accumulation curves for all nine ROV dives for sampling effort. Grey curve shows the grouped biotope sampling effort with 95% confidence intervals.

Figure 5. A Bathymetry map outlining the spatial distribution of biotopes per 50-meter annotation sample at each ROV dive site: a. Dive #1. b. Dive #2, c. Dive #3, d. Dive #4, e. Dive #7 and #8, f. Dive #9. g. Dive #10, h. Dive #13, with a pink star representing the biotope location and the individual biotopes outlined in their respective colours in the legend. Map contours derived from GEBCO bathymetry (GEBCO Bathymetric Compilation Group, 2022).

Figure 6. Non-metric multidimensional ordination of the benthic community at Rockall escarpment. The data were Hellinger transformed and the dissimilarity between sites (points) was assessed using a Bray-Curtis dissimilarity matrix. The grouping of the points indicates dissimilarity observed in the matrix, where sites that have similar species are plotted closer together in multidimensional space. Biotopes are clustered by colour, and the size of the point represents water depth.

List of Abbreviations

CWCs	Cold-Water Corals
ENAW	Eastern North Atlantic Water
IndVal	Indicator Values
MES	Marine Ecosystem Services
MPA	Marine Protected Area
NADC	North Atlantic Drift Current
NADW	North Atlantic Deep Water
nMDS	Nonmetric Multidimensional Scaling
POC	Particulate Organic Carbon
ROV	Remotely Operated Vehicle
SAC	Special Area of Conservation
SIMPER	Similarities Percentages
SORBEH	Slope Collapses on Rockall Bank and Escarpment Habitat
UPGMA	Unweighted Pair Group Method with Arithmetic Mean
VME	Vulnerable Marine Ecosystem

List of Appendices

7.1. Taxonomic identity of discriminating species identified by the SIMPER and IndVal analysis.

7.2. Output of the SIMPER analysis grouped by biotope

7.3. Output of the IndVal analysis grouped by biotope

7.4. Comparison of fusion levels derived from the UPGMA clustering dendrograms \log_{x+1} and Hellinger transformed species matrix.

1. Introduction

Described as being one of the last great wildernesses of planet Earth, the deep sea represents waters >200 m, with over 62% of Earth's oceans lying deeper than 1000m (Roberts, 2002). In the past, the depths of the ocean have largely been shrouded in the unknown, with the largest biome on Earth remaining the least explored because of difficult and costly access (Kazanidis et al., 2020). Continued exploration suggests that this vast environment supports a rich variety of life, the presence and actions of which are essential to multiple Marine Ecosystem Services (MES) and processes (Selig et al., 2019). MES, directly and indirectly, serve to benefit human well-being, for example, through the production of goods such as food (Kremen, 2005; Naidoo et al., 2008). However, marine ecosystem functions help contribute to benefits associated with climate regulation, as well as genetic and medicinal resources (Beaumont et al., 2007). Furthermore, they provide ecological resilience and resistance of communities to disturbances that ensure the delivery of services over time (Levin & Lubchenco, 2008).

Apart from adapted communities that rely on chemosynthesis for energy, the deep-sea ecosystem largely relies on oceanic primary production, acting as an energy source by transferring particulate organic carbon (POC), from the pelagic environment to the benthos (benthic-pelagic-coupling) (Johnson et al., 2018). Oceanic processes mix and drive the physical state of the overlying water column to facilitate the transport of POC to the bottom substrate (Griffiths et al., 2017). POC is crucial within benthic habitats for functions from nutrient cycling to energy transfer in food webs (Griffiths et al., 2017).

A habitat represents the environmental conditions that are capable of supporting a biological community (Brown et al., 2011). They may be defined by a combination of environmental factors (e.g., depth, slope) and biotic factors (e.g., food availability) (Allcock and Johnson, 2019). Climate change is currently one of the greatest threats to marine habitats and will have multiple ramifications. For example, changes in ocean biogeochemistry will likely affect the integrity and stability of habitats, by altering the seasonal patterns, location and composition of POC flux in the North Atlantic (Johnson et al., 2018). Circulation patterns in the North Atlantic, and their respective physical and chemical properties, are also expected to experience changes due to climate change because of increased stratification caused by warmer surface waters (Helm et al., 2011). Projected alterations to ocean circulation will likely limit oceanic productivity, biodiversity, and the distribution of deep-sea fauna because of warming, acidification and deoxygenation of deep waters (Morato et al., 2020). Evidence suggests the impacts of climate change are already evident as changes in the geographic distributions of marine species are already occurring (Johnson et al., 2018; Pinsky et al., 2020). With shifting baselines already occurring, it is crucial to investigate deep-sea habitats as we too often have only limited data against which to monitor changes.

Identifying and describing biotopes serve as a necessary basis for management and conservation, with biotopes representing specific assemblages of species described based on their dominant species (Dimitrakopoulos & Troumbis, 2019; Arya et al., 2022; Gonzalez-Mirelis & Buhl-Mortensen, 2015). This approach allows for comparison across geographic regions larger than the sum of one study (Davies et al., 2015).

Understanding the spatial distribution of biotopes is also an essential process for the implementation of regional spatial management tools, such as Marine Protected Areas (MPAs) (Davies et al., 2015). It can also serve as a foundation for potential monitoring and detection of future environmental change (Kuhnz et al., 2022). The concept of a biotope can also be employed to investigate questions related to ecological niches, the relationship between biodiversity and ecosystem processes, and the applied problems of nature conservation with ongoing climate threats (Dimitrakopoulos & Troumbis, 2019).

Deep-sea biotopes present within the North Atlantic are vital for the well-being of the global ocean environment and as such, have gained increasing attention from both an ecological and conservation perspective (Levin et al., 2019). While there are numerous marine organisms belonging to different deep-sea biotopes, the focus of this thesis will be on the most vulnerable, cold-water corals, sponges, and bioturbators. The Northeast Atlantic harbours thriving scleractinian cold-water corals (CWCs), occupying habitats at the top of seamounts, canyons, banks, and mounds (Hebbeln et al., 2019). CWCs are ecosystem engineers; organisms that create, modify, or destroy physical habitats, and are responsible for altering resource availability for other organisms (Jones et al., 1997). CWCs are also responsible for a positive feedback loop by not only increasing habitat heterogeneity and species richness at a landscape level but also causing abiotic changes (e.g. attenuating wave action) favourable to ecosystem engineers themselves (Jones et al., 2010; Romero et al., 2015; Wright et al., 2004). Due to the longevity and slow growth rates of CWCs, the recovery from disturbances will be very slow, if at all, making them especially vulnerable to changes in ocean climate

(Cheung et al., 2021; Huvenne et al., 2016). Effects from climate change such as the rise in carbon dioxide emissions, deoxygenation, and the warming and reduction of seawater pH, will be detrimental to corals (Arndt et al., 2010; Hebbeln et al., 2020; Solomon et al., 2007). Through testing the effect of increasing pH on the coral *Desmophyllum pertusum*, it is estimated that by the year 2100, ocean acidification may increase the susceptibility of the cold-water coral structure to bioerosion and mechanical damage (Hennige et al., 2015). This fragility in the coral framework could be further compounded by ocean climate driven changes to their food supply (Büscher et al., 2017).

Sponges (Porifera) are another important component of deep-sea ecosystems (Pawlik & McMurray, 2020). They are highly diverse concerning their morphology and symbiotic microbes and form one of nature's richest sources of novel secondary metabolites (Pawlik & McMurray, 2020; Pawlik & McMurray, 2020). Sponges that have a three-dimensional framework also can disrupt the layer of flowing seawater above a benthic substrate, referred to as boundary flow, by their positioning on the seabed (Culwick et al., 2020). The 3-D structure of the sponges allows commensal invertebrates such as shrimp and brittlestars, to filter feed away from the benthic boundary flow and the turbidity across the more complex substrate created by the sponge body re-suspends food particles (Culwick et al., 2020). However, little is known about the physiological effects on deep-sea sponges or the ecological response (e.g. distribution shifts) to a changing ocean climate (Samuelson et al., 2022).

Bioturbators, including benthic organisms such as urchins and starfish, are another example of ecosystem engineers (Mermillod-Blondin & Rosenberg, 2006). By reworking the sediment, they are responsible for enhancing the redistribution of organic matter, nutrients, and oxygen and the remineralization of organic matter in the burrows (Smith et al., 1993). With a changing environment caused by climate change (e.g. water column declines) a reduction in bioturbation rates is expected (Levin et al., 2009; Smith et al., 1997, 2000; Sweetman et al., 2017). Solan et al. (2004) found that bioturbation decline generally leads to biodiversity loss. However, the magnitude of species loss depends on the species' life traits and their resilience to environmental impacts (Solan et al., 2004). Sites with high macrofaunal species richness and high community bioturbation showed the highest decline in ecosystem functions and the slowest recovery (Lohrer et al., 2004).

The first step in understanding how climate change may affect biotopes and species of ecological importance is to describe their composition and spatial patterns. As such, the objective of this study is to build a baseline describing the megabenthic composition of biotopes present along the Rockall Escarpment, on the eastern side of Rockall Bank, Northeast Atlantic. The Rockall Bank hosts many vulnerable cold-water corals and sponges, in addition to Marine Protected Areas. As such, it is important to understand the biotope composition along with their spatial distribution, to refine the boundaries of Marine Protected Areas in the near future.

2. Methods

2.1 Study Area

Rockall Bank is a submerged microcontinent, located close to Hatton Basin and Hatton Bank to the northwest. It is further separated from Scotland's continental margin by Rockall Trough (Roberts, 1971,1975). It hosts a number of MPAs and Special Areas of Conservation (SAC) that were once areas heavily fished and now benefit from bottom-fisheries closures (Weaver & Johnson, 2012). The Hatton Bank SAC, the North West Rockall Bank SAC, the East Rockall Bank SAC as well as the Hatton Rockall Basin Nature Conservation MPA, are designated SACs under the 2010 Marine Act (Johnson et al., 2019). The Hatton Rockall Basin Nature Conservation MPA consists of substrate of sedimentary mud and coarse sand with exposed bedrock, boulders, and cobbles (Roberts et al., 2008). It displays a wide range of habitats and a diverse burrowing and encrusting faunal assemblage that includes long-lived and fragile deep-sea coral gardens and sponge aggregations (Roberts et al., 2008). Within these SACs, areas of fine sand scarred by iceberg plough marks have exposed rubble fringe areas colonized with the coral-water coral *D. pertusum* (Howell et al., 2009). In addition, the eastern flanks of Rockall Bank, the Franken Mound area on western Rockall Bank, and the deeper Rockall Trough, have also been characterized by large mounds of *D. pertusum* reefs (Howell et al., 2009; Robert et al., 2014; Gage, 1986). The sea urchin *C. cidaris* has also been reported, in high densities, in sandy sediments within the surrounding areas of Rockall Bank (Gage, 1986) as well as in coral rubble fields (Howell, 2010; Robert et al., 2014). Unfortunately, the past deep-water trawl fishery severely impacted the Hatton-Rockall plateau CWCs and sponges in the area, resulting in deep-sea corals and sponge aggregations being regarded as vulnerable marine ecosystems (VMEs) (Johnson et al., 2019). In the future, these species will additionally

be threatened further by climate change and ocean acidification (Perez et al., 2018; Roberts et al., 2016; Roberts & Cairns, 2014).

Rockall is characterized by a complex oceanography, where circulation in the area is characterized by numerous eddies (Holliday et al., 2000). It is surrounded by multiple water masses including the North Atlantic Drift Current (NADC), Eastern North Atlantic Water (ENAW) and North Atlantic Deep Water (NADW) (Howe et al., 2006). Upper layers of water fall within the temperature-salinity range of ENAW and are more saline than the subpolar waters lying below (Harvey, 1982). The NADW lies below the ENAW at a depth past 1200m (Howe et al., 2006). The salinity of the underlying water is typically associated with a combination of Labrador Sea Water, Norwegian Sea Deep Water and Antarctic Bottom Water (Howe et al., 2006). Rockall is influenced by prominent shelf edge currents along the European continental shelf break, contributing to the flow of warm and saline upper waters with the ENAW (Huthnance, 1986). Water masses in this area are highly stratified with different salinities, oxygen contents and velocities (New & Smythe-Wright, 2001; Holliday et al., 2000; Read, 2000).

2.2 Data Collection

In July of 2014, the Celtic Explorer CE14011 "Slope Collapses on Rockall Bank and Escarpment Habitats" (SORBEH) expedition deployed the *Holland I* remotely operated vehicle (ROV) at nine dive sites, with dive nine divided into two parts (a and b) (Table 1). Using the ROV, video transects were obtained and used for further analysis. The expedition surveyed a submarine landslide headwall scarp present within

the Rockall Bank Slide Complex (Georgiopoulou et al., 2013), previously mapped using a multibeam echo sounder Simrad EM120 (11.75-12.75 kHz, deeper than 200m) and Simrad EM1002 (shallower than 200m) (Sacchetti et al., 2011). The ROV *Holland I* was equipped with an OE 14366 colour zoom video camera (1920 x 1080 pixels). Digital stills were also taken roughly every 40 seconds using an oblique mounted downward-looking Kongsberg OE14-208 camera with a focal length of 7.188 mm and a maximum aperture of f/2 to aid in species identification (Robert et al., 2014). To obtain a standardized sampling unit, each dive transect was split into sampling units of 50 m in length, referred to as “samples”.

All epibenthic megafauna larger than 2 cm observed in video were identified and counted by expert annotators using local species ID catalogs. Annotation is the process whereby the contents of images and video (i.e., organism IDs, substrate, depth) are counted and analyzed, to be considered in subsequent scientific analysis (Schoening et al., 2016). Species identification from imagery is challenging, thus the use of morphospecies is used to support consistent naming of organisms (Howell et al., 2019). Such an approach is commonly used in benthic studies using imagery to help ensure consistent labelling of organisms (Howell et al., 2019). A description of morphospecies labels for discriminating species discussed in this research project along with their lowest possible taxonomic identity is supplied in appendix 7.1. The total abundance of each morphospecies observed within each 50 m sample was tallied to create a morphospecies by sample matrix along with sample metadata (e.g., geolocation and

depth).

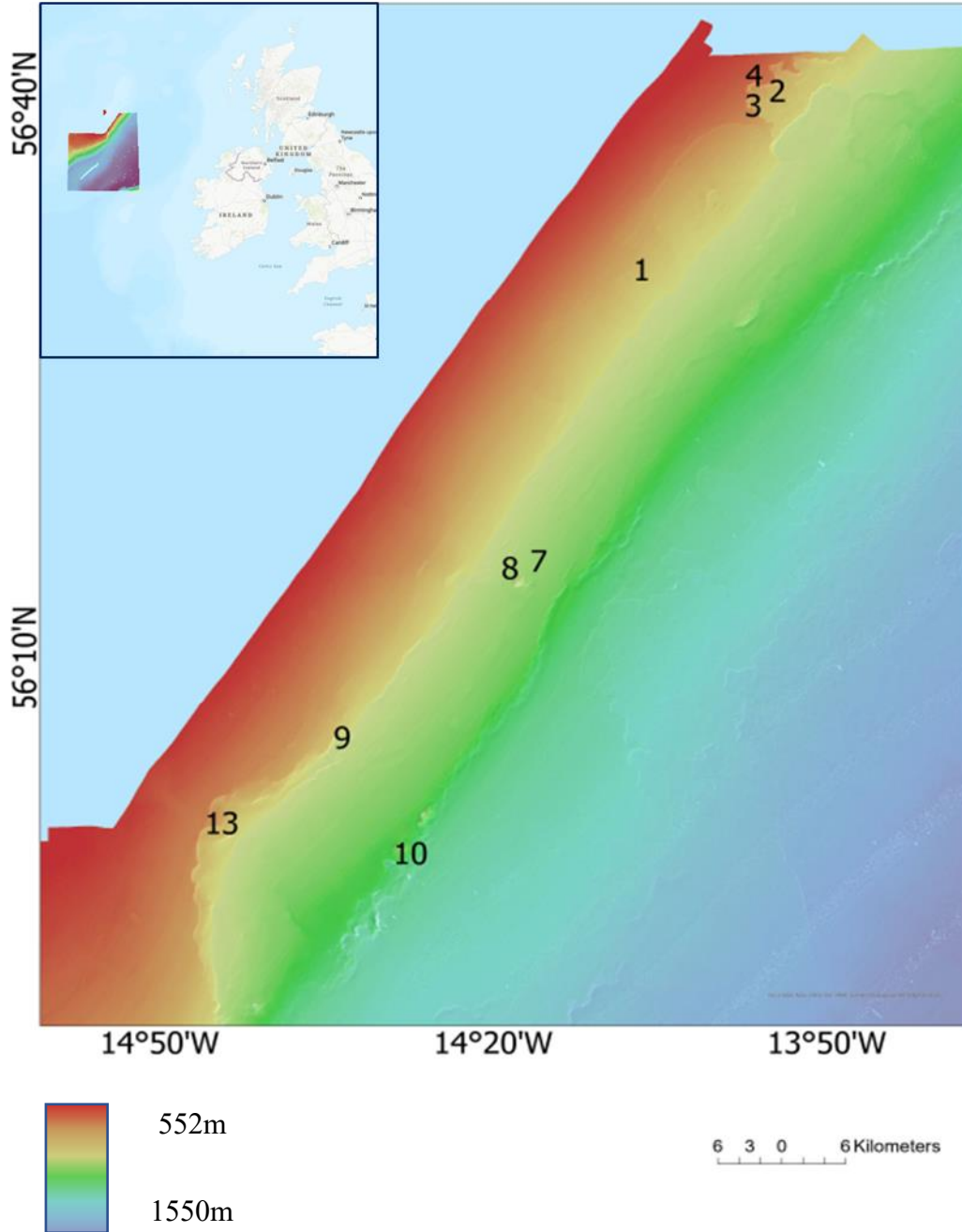


Figure 1. Multibeam bathymetry map of the full study site with the locations of the nine ROV dive sites across the Rockall escarpment. Map projection is UTM zone 28N.

Table 1. Summary of ROV dives and video transects assessed.

ROV Dive Number	Start Date	Start Time GMT	Start Lat N	Start Long W	Start Water Depth (m)	End Date	End Time GMT	Geomorphology
1	17/07/2014	06:08:00	56° 30.1500	14° 6.7130	723	17/07/2014	12:00:00	Small intra-landslide scarp
2	17/07/2014	19:53:00	56° 39.6760	13° 53.9937	552	18/07/2014	01:30:00	Steep slide wall in the northern scar
3	18/07/2014	04:12:00	56° 40.0404	13° 53.9870	677	18/07/2014	11:09:00	Steep wall in landslide scar
4	18/07/2014	17:46:00	56° 40.4487	13° 55.0494	593	19/07/2014	00:50:00	Northern headwall scar
7	20/07/2014	04:09:00	56° 14.4261	14° 16.4401	1080	20/07/2014	12:20:00	Ridge of Volcanic Mount
8	20/07/2014	20:36:00	56° 13.9801	14° 18.0446	1033	21/07/2014	05:49:00	Pinnacle ridge, base of isolated pinnacle, lava outcrop and flow
9a	21/07/2014	20:52:00	56° 3.9005	14° 33.9968	950	22/07/2014	05:34:00	First side of shallow and wide along slope ridge-and-moat
9b	21/07/2014	20:52:00	56° 3.9005	14° 33.9968	950	22/07/2014	05:34:00	Second side of shallow and wide along slope ridge-and-moat
10	22/07/2014	13:17:00	55° 58.5910	14° 29.1220	1550	23/07/2014	05:38:00	Isolated pinnacle and an adjacent small slide scar
13	25/07/2014	06:01:00	56° 0.2755	14° 46.1216	648	25/07/2014	07:51:00	No geomorphic feature found

2.3 Statistical Analysis

Following the methods outlined in Borcard et al. (2011), a multivariate analysis was performed to classify the benthic community abundance and structure observed on the Rockall escarpment. The data were transformed prior to analysis in order to minimize the skewness associated with the high abundance of specific morphospecies and make dissimilarities between samples double-zero asymmetrical (Legendre & Borcard, 2018). The performed distance transformations included $\log x+1$, Chord and Hellinger transform with Bray Curtis dissimilarity matrix. Using the “vegdist”, “decostand” and “metaMDS” functions in the R package *vegan*, a visualization of the annotation data was undertaken based on multiple transformation methods (e.g., $\log x+1$, Chord and Hellinger transform with Bray Curtis dissimilarity matrix) using a two-dimensional nonmetric Multidimensional Scaling (nMDS) (Borcard et al., 2011). Both a stress and a goodness of fit plot were created to evaluate how the transformed data were grouped within multivariate space.

Since both the Hellinger transformation and $\log x+1$ transformation evaluated with the Bray Curtis dissimilarity matrix demonstrated almost identical stress values of less than 0.2, the hierarchical clustering analyses were performed for both using the function “hclust” in *vegan*. Cluster analysis allows one to measure the distance between pairs of objects and then to group the objects that are closer together. Visualization of the hierarchical relationships is achieved using a dendrogram, a tree-like representation of the data (Jin Chen et al., 2009; Murtagh, 1984). Various clustering methods were explored, including single linkage agglomerative clustering, complete-linkage

agglomerative clustering, Unweighted Pair Group Method with Arithmetic Mean (UPGMA) agglomerative clustering, centroid clustering and ward's minimum variance (D2) clustering. To determine the most appropriate clustering method, a Cophenetic correlation was used to derive Pearson's r correlation between the dissimilarity matrix and the cophenetic matrix (Borcard et al., 2011).

Fusion levels were used to depict dissimilarity values where fusion between two branches of a dendrogram occurred. Subsequent plotting of these fusion levels helped define cutting levels in the dendrogram (Borcard et al., 2011) and were used to classify the terminal nodes. To characterize the dominant morphotaxa in each cluster and identify the species driving the differences between clusters, both SIMPER (see Appendix 7.2) and IndVal analyses (see Appendix 7.3) were used. SIMPER indicates which species, along with their presence and relative abundance, contribute to the dissimilarity within cluster groups (Clarke and Gorley, 2015), while the species Indicator Values (IndVal) combines species mean abundances and the frequency of occurrences in the groups, in order to observe the most prominent members of the clusters known as indicator species (Borcard et al., 2011). Both SIMPER and IndVal are commonly used methods to define which taxa drive changes in benthic community structure (Borcard et al., 2011).

Species accumulation curves were used to evaluate whether sampling effort was adequate to capture megabenthic community composition within each resultant biotope, from the cluster analysis, and compare species richness across biotopes. Reaching the asymptote of species accumulation curves is indicative that sufficient seabed imagery

was obtained to capture the majority of occurring taxa within that biotope (Borcard et al., 2011).

3. Results

3.1 Megafaunal community structure

In total, 59,418 individual organisms representing 199 megafaunal morphospecies were analyzed. Cnidaria was the most diverse phylum representing eighty morphotaxa and 40% of all species. The most abundant species of cnidarians was the reef-building cold-water coral *S. variabilis*, annotated 2,835 times. Echinodermata followed as the second most diverse phyla with fifty-two morphotaxa identified, accounting for 26% of all species present. This was mostly associated with the echinoderms *Araesoma fenestrum*, annotated 9,618 times, and an unidentified brittle star *Ophiuroidea* sp. 4 annotated 7,798 times. Thirty-eight morphotaxa from the phylum Porifera were recorded, accounting for 19% of all species. The most abundant morphotaxa within the phylum Porifera was the class Demospongiae, annotated 4,480 times. Representing 5% of all taxa, ten morphotaxa belonging to the phylum Arthropoda were observed. The most abundant morphotaxa in this phylum belonged to the super family Galattheoidea annotated 502 times. Phylum Chordata possessed nine morphotaxa accounting for 4.5% of all morphotaxa with the most abundant taxa being Tunicates, annotated 571 times. Possessing three morphotaxa, Mollusca accounted for 1.5% of all taxa. The most prominent morphotaxa was Buccinidea. Bryozoa possessed two morphotaxa, accounting for 1% of the taxa observed, mainly a morphotaxa of the genus *Reteporella*. This was additionally seen for Annelida accounting for 1% of the taxa

being echiurans. One morphotaxa, Paguridae, was found within the phylum Crustacea, accounting for 0.5% of all species present.

The highest cophenetic correlation value of 0.86 was obtained by the UPGMA clustering method with a Hellinger and Bray Curtis dissimilarity matrix. Assessment of fusion levels compiled from the dendrogram suggested that seventeen or twelve cluster groups were present (see Appendix 7.4). Coercing the dendrogram into seventeen cluster groups resulted in multiple single station nodes that were unlikely representative of broader prominent biotopes. Selecting twelve clusters removed the most single station groups and through further assessment of discriminating species contributing to the dissimilarity, supported the ecological relevance of that number of clusters, referred to herein as biotopes (Figure 2).

Both SIMPER and INDVAL showed agreement in the most abundant species (Figure 3); however, IndVal promoted individual species that were rarer. A description of the biotopes (i.e., discriminating species, number of samples, distance, dives, substrate, and depth range) is given in Table 2. Biotopes seven and ten demonstrated single species biotopes and were examined manually as both SIMPER and IndVal require a minimum of two terminal nodes present in a group to successfully run.

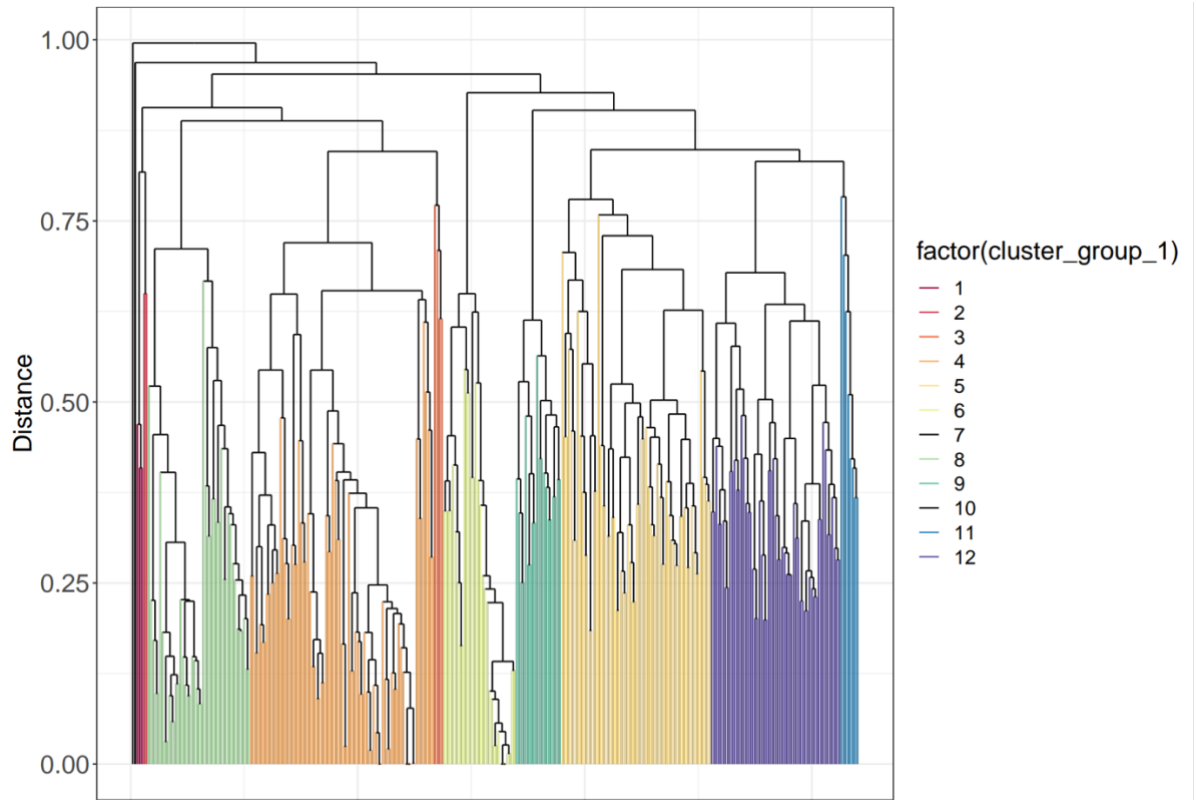


Figure 2. UPGMA hierarchical clustering dendrogram by Hellinger and Bray-Curtis dissimilarity matrix depicting the resultant 12 coloured biotope clusters.

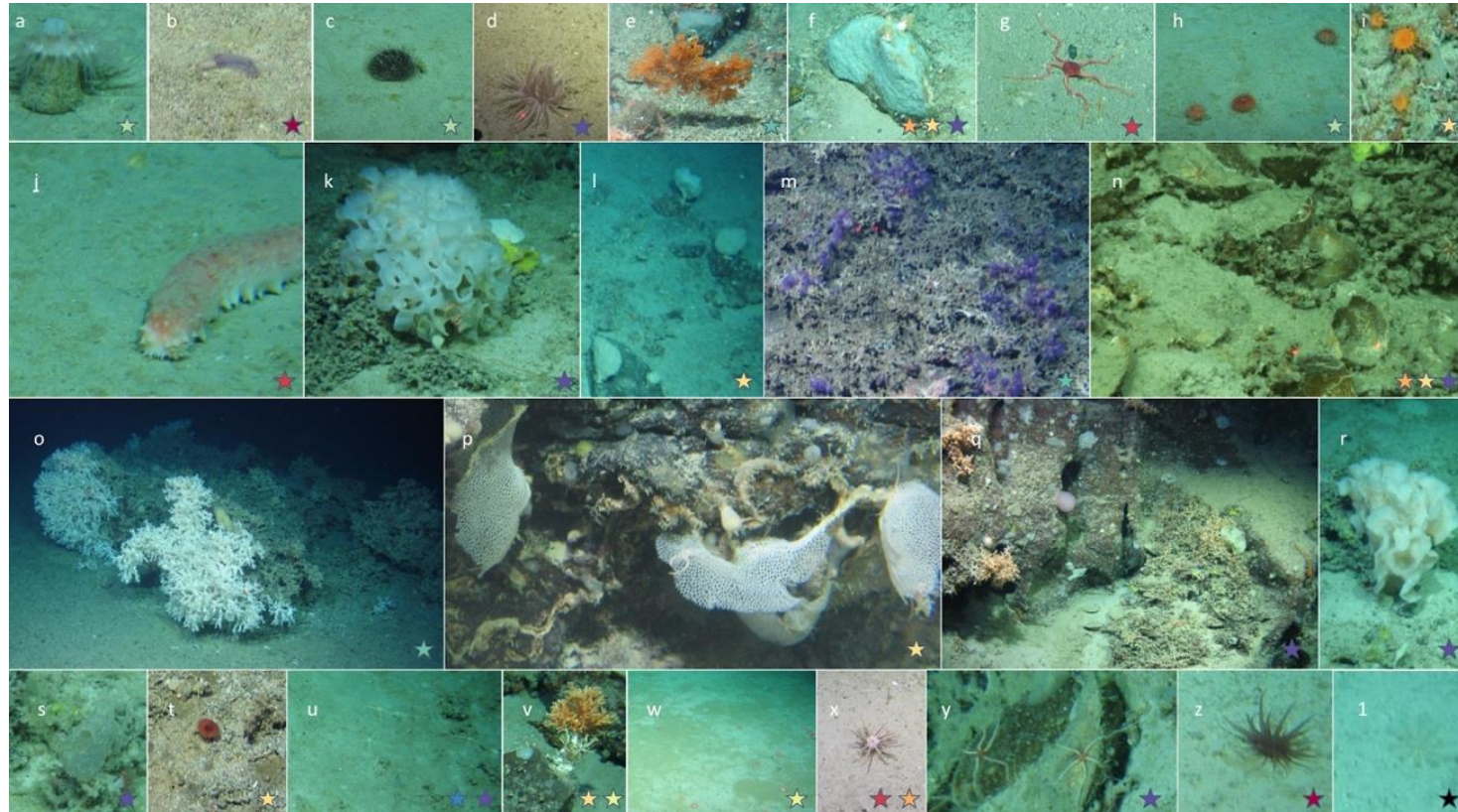


Figure 3. Images of the discriminating morphotaxa for each biotope (stars): a. Anthozoa species 1, b. Holothuroidea species 4, c. Echinozoidea species 2, d. Anthozoa species 14, e. Leiopathes species, f. Demospongiae, g. Ophiuroidea species 1, h. Echinozoidea species 1, i. Anthozoa species 8, j. *Parastichopus* species, k. *Asconema foliatum*, l. Phakellia, m. Flabellidae, n. Demospongiae, o. *Desmophyllum pertusum*, p. Reteporella, q. Porifera species 6, r. Porifera species 3, s. Ascidiacea, t. Anthozoa species 6, u. Ophiuroidea species 2, v. *Madrepora oculata*, w. *Araesoma fenestratum*, x. *Cidaris cidaris*, y. Ophiuroidea species 4, z. Anthozoa species 5 and 1. Crinozoidea species 2.

Table 2. Biotope summary table with discriminating species resulting from both SIMPER and IndVal.

Biotope Number	SIMPER Discriminating Species*	IndVal Discriminating Species*	Number of Samples	Distance (m)	Dive	Dominant Substrate (general)	CATAMI Classification of Substrate	Depth min-max (m)
1	Holothuroidea species 4, Anthozoa species 5	Holothuroidea species 4, Anthozoa species 5, Anthozoa species 12	3	150	9	Soft	Sediment	848.46- (854.31)- 858.11
2	Ophiuroidea species 1, Ophiuroidea species 3, Cerianthidae species 1, <i>Parastichopus</i> species, <i>Cidaris cidaris</i>	Ophiuroidea species 1, Ophiuroidea species 3, <i>Liponema brevicorne,</i> <i>Epizoanthus paguriphilus</i>	2	100	9	Mixed	Sediment and pebbles	833.07- (843.66)- 854.25
3	<i>Parastichopus</i> species, Anthozoa species 4, Holothuroidea species 1, Cerianthidae species 1, <i>Calveriosoma hystrix</i>	<i>Parastichopus</i> species	4	200	9, 2	Soft	Sediment	573.39- (713.48)- 851.96
4	<i>Cidaris cidaris,</i> Cerianthidae species 1, Demospongiae, Holothuroidea species 3	<i>Cidaris cidaris</i>	81	4050	2, 3, 4, 9, 13	Mixed	Sediment and pebbles	443.55- (620.98)- 868.29
5	Demospongiae, Anthozoa species 8, <i>Madrepora oculata,</i> Phakellia species 1, Anthozoa species 14, Galattheoidea, Reteporella, Holothuroidea species 3,	Demospongiae, Anthozoa species 8, <i>Madrepora oculata,</i> Phakellia species 1, Galattheoidea, Reteporella, Anthozoa Species 6	66	3300	7, 8, 9, 10	Hard	Boulders	770.2- (977.98)- 1258.35

Biotope Number	SIMPER Discriminating Species*	IndVal Discriminating Species*	Number of Samples	Distance (m)	Dive	Dominant Substrate (general)	CATAMI Classification of Substrate	Depth min-(mean)-max (m)
5	Phakellia species 2, Anthozoan species 6		66	3300	7, 8, 9, 10	Hard	Boulders	770.2- (977.98)- 1258.35
6	<i>Araesoma fenestrum</i> , <i>Madrepora oculata</i>	<i>Araesoma fenestrum</i>	32	1600	9	Mixed	Boulders and sediment	746.62- (841.94)- 944.91
7	NA (Manually assessed Cnidarian species 6)	NA (Manually assessed Cnidarian species 6)	1	50	9	Hard	Bedrock exposed	935.55
8	Echinoidea species 1, Anthozoa species 1, Echinoidea species 2	Echinoidea species 1, Anthozoa species 1, Echinoidea species 2	45	2250	1, 2	Soft	Sediment	659.27- (701.18)- 727.72
9	<i>Desmophyllum pertusa</i> , Family Flabellidae, Class Asteroidea, Leiopathes species	<i>Desmophyllum pertusa</i> , Family Flabellidae, Callogorgia species 1, Chaceon species 1, <i>Flabellum alabastrum</i> , Class Asteroidea, Decapoda, Leiopathes species	20	1000	7, 8	Mixed	Sediment and Cobbles	857.65- (882.22)- 913.16
10	NA (Manually assessed Crinoidea species 2)	NA (Manually assessed Crinoidea species 2)	1	50	10	Soft	Sediment	1550.04
11	Ophiuroidea species 2, Cerianthidae species 1	Ophiuroidea species 2	8	400	10	Mixed	Sediment and fine pebbles	1278.17- (1503.11)- 1560.22
12	Anthozoa species 14, Ophiuroidea species 4,	Anthozoa species 14, Parantipathes, <i>Asconema</i> <i>foliatum</i>,	57	2850	10	Hard	Boulders	1192.56- (1402.19) - 1558.02

Biotope Number	SIMPER Discriminating Species*	IndVal Discriminating Species*	Number of Samples	Distance (m)	Dive	Dominant Substrate (general)	CATAMI Classification of Substrate	Depth min-(mean)-max (m)
12	<i>Solenosmilia variabilis</i> , Parantipathes , <i>Asconema foliatum</i> , Demospongiae , Cerianthidae species 1, Ophiuroidea species 2, Ascidiacea , Porifera species 6 , Porifera species 11, Demospongiae, Porifera species 3 , Holothuroidea species 1, Ophiuroidea species 4	Porifera species 6 , Ascidiacea , <i>Solenosmilia variabilis</i> , Ophiuroidea species 4 , Brisingida species 1, Porifera species 5, Pentametrocrinus, Anthozoa species 9, Demospongiae , Crinoidea species 1, Actinoscyphia, Porifera species 6, Porifera species 3 , Shrimp species, <i>Aplysilla sulfurea</i>	57	2850	10	Hard	Boulders	1192.56-(1402.19) - 1558.02

*Agreed discriminated species of SIMPER and IndVal in bold.

3.2 Biotope description

Biotope one was found on unconsolidated soft sediments. The species that contributed the most to the differentiation of this biotope was the *Holothuroidea* sp. 4. Other important species included an anemone in the Order Actiniaria. The community was found across a small area in quite a narrow depth range (848 m - 858 m) of dive #9 (Table 2), which followed a shallow and wide slope ridge-and-moat.

In biotope two, *Ophiuroid* sp.1 and *Ophiuroid* sp.3 were prominent, along with other soft sediment taxa (e.g cerianthids, pom-pom anemones, and the urchin *C. cidaris*). However, SIMPER suggested the presence of the cold-water coral *Parastichopus* sp. was also important in defining the biotope. The depth range for this biotope (833 - 854 m) overlapped with that of biotope one but tended to occur on a mixed unconsolidated substrate as seen on the shallow and wide along slope ridge-and-moat of dive #9.

Biotope three predominantly occurred on the sediment dominated areas of dives #2 and #9. SIMPER and indVal both agreed on the cold-water coral *Parastichopus* sp. as the taxa responsible for differentiating between other biotopes. Anthozoans (anemones) of the order Actiniaria, the sea cucumber *Holothuroidea* sp.1, tube-dwelling anemones *Cerianthidae* sp.1 and the urchin *Calveriosoma hystix* were also prominent in biotope three. The depth range was 573.39 - 851.96 m and dominated throughout dives #2 and #9.

Biotope four had a mixed substrate of sediment and pebbles between a depth of 443.55 - 868.29 m. The morphospecies that were important contributors were the urchins *C. cidaris*, Cerianthidae sp.1, Demosponge and Holothuroidea sp.3. The depth range of this biotope was larger than for biotopes one, two and three at 443.55 - 868.29m. Biotope four was sampled 81 times (4050m) and species accumulation curves showed it to be approaching the asymptote, suggesting that it was likely sampled adequately (Figure 4).

Biotope five was characterized by Anthozoans (anemones) in the family Actinostolidae, Demosponge, crustaceans in the class Malacostraca, and the cold-water coral *M. oculata*. Additionally, lamellate, cup-shaped sponges likely in the family Phakellia, and lace corals (Bryozoa, likely Reteporella) were prominent discriminating taxa. This biotope characterized 66 samples (3300m) at a depth range of 770.2 - 1258.35m. Biotope five was dominant in dives #7, #8, #9 and #10 with a hard substrate consisting of boulders. While biotope five did exhibit one of the highest species richness, accumulation curves suggested that the biotope remained under sampled (Figure 4).

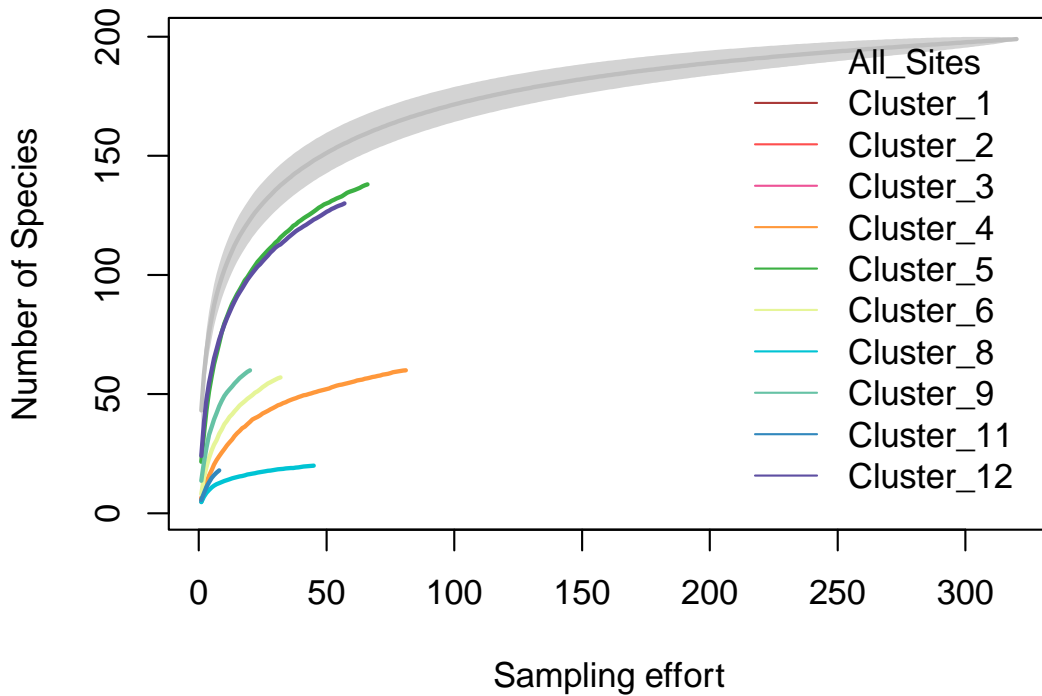


Figure 4. Species accumulation curves for all nine ROV dives for sampling effort. Grey curve shows the grouped biotope sampling effort with 95% confidence intervals.

Biotope six occurred across 32 samples within a wide depth range (746 - 944 m) but was only present in the sediment and pebble substrate of dive #9. It was discriminated by the urchin *A. fenestrum* occurring in sediment patches in between boulders occupied by the cold-water coral *M. oculata*.

Biotope seven was a single sample biotope characterized by a monospecific anemone patch (Cnidarian sp.6) found in dive #9 and occurring on an exposed patch of bedrock at 935 meters.

Biotope eight was predominantly found on sediment at a depth range of 659.27 - 727.72m. The Echinoidea sp.1 (urchin) contributed most to the differentiation of the biotope while Echinoidea sp.2 (urchin) and a Cnidarian in the order Actiniaria (anemones) were also important. Biotope eight was mostly found in dives #1 and #2, characterized by a landslide scarp and a steep slide wall (Figure 5).

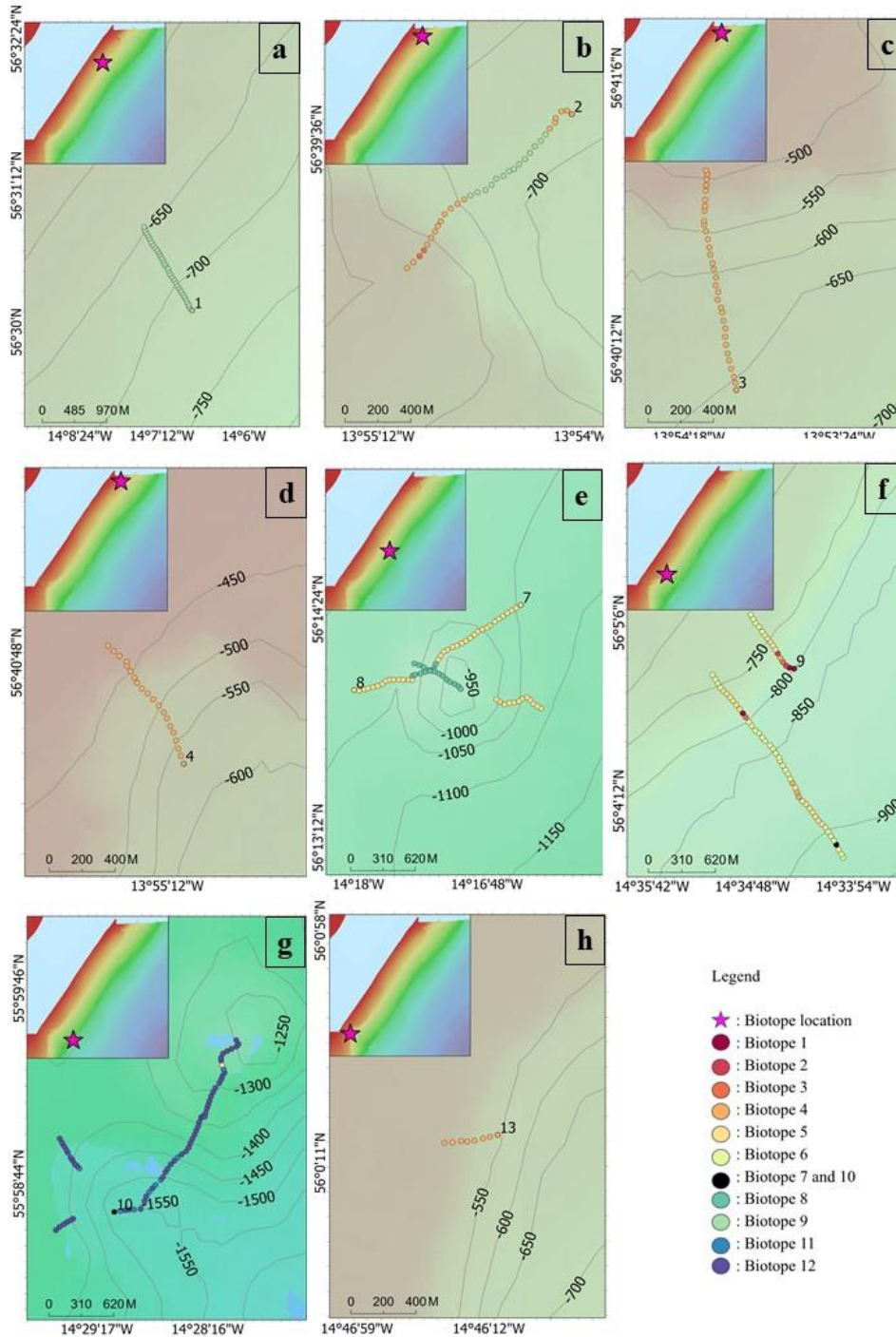


Figure 5. A Bathymetry map outlining the spatial distribution of biotopes per 50-meter annotation sample at each ROV dive site: a. Dive #1. b. Dive #2, c. Dive #3, d. Dive #4, e. Dive #7 and #8, f. Dive #9, g. Dive #10, h. Dive #13, with a pink star representing the biotope location and the individual biotopes outlined in their respective colours in the legend. Map contours derived from GEBCO bathymetry (GEBCO Bathymetric Compilation Group, 2022).

Biotope nine was characterized by *D. pertusum* as a discriminating species that shaped this biotope. However, a cup coral of the family Flabellidae, a seastar (Asteroidea) and a black coral in the genus *Leiopathes* also contributed to its differentiation. This biotope occurred within a depth range of 857.65 - 913.16 m in a mixed substrate of sediment and cobbles. Biotope nine was found throughout dives #7 and #8 along the ridge of a volcanic mount as well as a pinnacle ridge and lava outcrop and flow. Species accumulation curves showed biotope nine to be approaching the asymptote suggesting it was adequately sampled.

Biotope ten was a single sample biotope characterized by a feather star (Crinoidea sp.2), occurring on sediment at 1550.04 meters.

Biotope eleven was marked by having the deepest mean depth across biotopes (see Table 2) and dominated by brittle stars (Ophiuroidea sp.2) and tube-dwelling anemones (Cerianthidae sp.1). Cerianthidae sp.1 was observed to be the most abundant discriminating species (reported 2907 times) while the Ophiuroidea sp.2 was agreed upon by SIMPER and IndVal as the species contributing most to its differentiation. The biotope was found at a depth of 1278.1 - 1560.22 m within sediment and fine pebbles. It was prominently found in dive #10 that covered an isolated pinnacle and an adjacent small slide scar.

Biotope twelve was differentiated by the largest number of discriminating species. Anemones (Actiniaria), brittle stars (Ophiuroidea sp.4), the cold-water coral *S. variabilis*, a black coral in the genus *Parantipathes*, the Venus flower basket sponge (Euplectella), other unidentified Demospongiae (Porifera sp.6 and Porifera sp.3) and

Tunicates, are just some of the discriminating morphospecies agreed upon by SIMPER and IndVal. This biotope was found in deeper areas, between 1192.56 - 1558.02 m. Biotope twelve was found in dive #10 which surveyed an isolated pinnacle and an adjacent small slide scar. The substrate was composed primarily of boulders. Biotope twelve suggested a high species richness, however, accumulation curves indicated that the biotope was under sampled (Figure 4).

The nMDS ordination plot showed an association between water depth and biotopes (Figure 6). Biotopes eleven and twelve were present at the greatest depths (below ~1200 m). On the other hand, biotopes four and eight occurred in shallower waters (~450m to 850m), while biotopes five, six and nine occurred in deeper waters (~750 to 1,200 m).

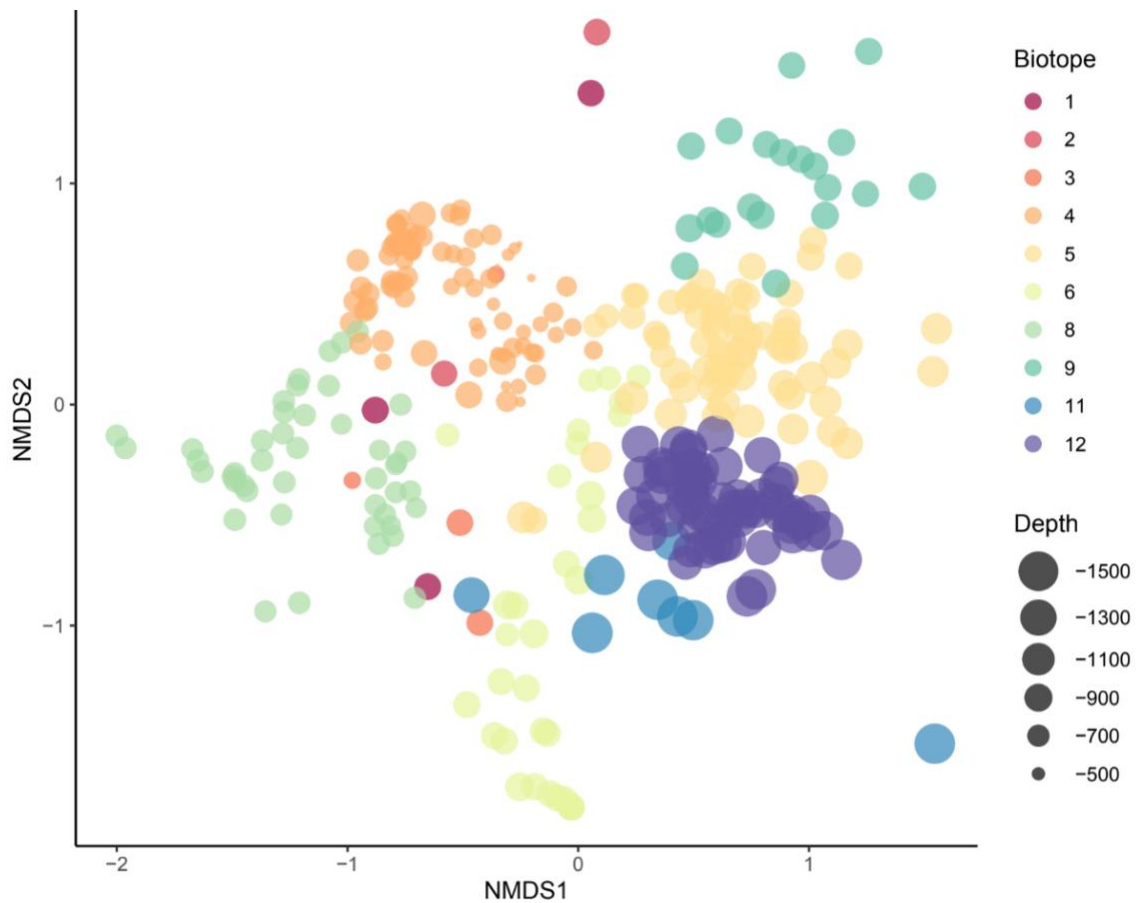


Figure 6. Non-metric multidimensional ordination of the benthic community at Rockall escarpment. The data were Hellinger transformed and the dissimilarity between sites (points) was assessed using a Bray-Curtis dissimilarity matrix. The grouping of the points indicates dissimilarity observed in the matrix, where sites that have similar species are plotted closer together in multidimensional space. Biotopes are clustered by colour, and the size of the point represents water depth.

4. Discussion

The objective of this baseline assessment was to describe the composition of the megabenthic biotopes present along the Rockall Escarpment. ROV video analysis of nine transects depicted that Cnidarians were the most diverse phyla followed by Echinodermata and Porifera. Twelve biotopes were identified and inhabited a mixture of substrates, but the more vulnerable sessile taxa, *S. variabilis*, *M. Oculata*, and *D. pertusum*, appeared on hard or mixed substrates.

Biotopes five, seven, nine and twelve, were largely defined by benthic taxa associated with hard substrates, with biotopes five and twelve displaying similar levels of morphotaxa richness. The biotopes defined by a larger number of discriminating species were only observed within dives #7, #8, #9 and #10. The focus of these particular dives captured habitats defined by complex bathymetry features, including ridges and mounds, close together in geographic space at the southern end of the Rockall Escarpment. The complex geomorphology associated with these benthic features provides a settling ground for epibenthic organisms such as CWCs (Wienberg et al., 2008). Isolated regions of elevated seafloor typically due to igneous activity (e.g. dive #7 and #8), lead to hard bottom substrate, which are particularly favourable for sessile suspension feeders (Mortensen et al., 2008). Geomorphology, such as ridges possessing plough marks of glacial origin, also create hard substrate (Rogers, 1999; Wilson, 1979a, 1979b; Fosså et al., 2002). Soft sediment fills the center of ridges while coarse debris forms at the edges of these features allowing for the colonization and settlement of vulnerable sessile taxa on the hard substrate (e.g CWCs and sponge communities) (Rogers, 1999; Wilson, 1979a, 1979b). Dives #8 and #9 were an appropriate representation of the geomorphology of these features while possessing a combination of soft and hard substrate throughout the area.

Complex geomorphology and its interaction with the water column (e.g., strong currents and turbidity) are an important factor in identifying suitable habitats for many benthic species (Price et al., 2019). Specifically, for coral taxa that depend on food supply mechanisms provided by deep-water bottom currents (Price et al., 2019). In the study region, three coral taxa that form a complex framework were characterized in

different biotopes along the Rockall Escarpment, these included *S. variabilis*, *M. oculata*, and *D. pertusum*. *S. variabilis* was a prominent characterizing taxa within biotope 12; a biotope associated with hard substrate, with a rich biodiversity, and discriminated by the largest number of morphospecies. *S. variabilis* typified a biotope with a deeper depth distribution (1100-1560 m), whereas the *D. pertusum* and *M. oculata* biotopes (biotopes five, six and nine) were constrained to shallower depths. *D. pertusum* and *M. oculata* have been found at shallower depths and across a greater range of productivity, which suggests the shallower biotopes could be more vulnerable to changes in particulate organic carbon or food input (Davies & Guinotte, 2011). *D. pertusum* and *M. oculata* have been reported in nearby areas on giant carbonate mounds at ~800 m depth at Rockall Bank by Oevelen et al. (2009), geographically constrained to surface productivity and the downslope transport of organic-rich surface water. Davies et al. (2015) additionally found *D. pertusum* and *M. oculata* at depths between 500-1200m associated with topographic features such as ridges and escarpments. The topographic features associated with *D. pertusum* and *M. oculata* were seen to be characterized by enhanced turbidity and high current velocities that enhance encounters with food particles (Davies et al., 2015). *D. pertusum* and *M. oculata* biotopes have been described on the southwest margin of Rockall Trough however at a shallower depth of ~750m compared to the average depth of ~895 m in which they were observed in this study (Bonneau et al., 2018). The urchins *A. fenestrum* and *C. cidaris* were also prominently co-occurring with *M. oculata*. *Cidaris cidaris* has also been identified as a dominant species in Rockall Bank whereby, it represented the most abundant echinoid along with *Echinus* cf. *acutus* (Wienberg et al., 2008). *Cidaris cidaris* was equally

observed to be a dominant species within our study, it was not however the most abundant species in the Rockall Escarpment. *Araeosoma fenestratum* was observed to be the most abundant species in our study within the boulders and sediment composition of the slope ridge-and-moat present within biotope 6. Compared to other studies performed within the area, *C. cidaris* was also present whereas *Echinus cf. acutus* was not.

Wienberg et al. (2008) reported the presence of *Echinus cf. acutus* to be present within areas of dense coral framework and coral debris which were not abundantly observed in our study allowing us to infer that perhaps surrounding environmental conditions (e.g., ocean acidification and water warming) with ongoing climate change may be impacting their distribution surrounding the Rockall Escarpment (Puerta et al., 2020).

4.1 Conservation

Climate change has the potential to greatly affect deep-sea ecosystems, particularly with respect to sessile benthic organisms such as CWCs (Przeslawski et al., 2008). As sessile organisms, they are attached directly to hard substrates and are restricted in their ability to directly escape unfavourable conditions (Przeslawski et al., 2008). Within the study area of Rockall Bank, a reduction of habitat suitability due to ocean acidification has already been observed for certain species, particularly *D. pertusum* (Puerta et al., 2020). Due to past harmful fisheries such as bottom trawling, the North-East Atlantic Fisheries Commission (NEAFC) has enforced the Hatton-Rockall closures with static gear for the protection of VMEs (Johnson et al., 2019). The NEAFC closures served to protect the main distribution of corals on the Rockall plateau however, there was much debate over the uncertainty in the boundaries of these closures (Johnson et al., 2019). The uncertainty caused by the lack of evidence and conflicting

reports of intensive fishing activity, lead to some MPAs having continued fishing activities (e.g. East Rockall) (Johnson et al., 2019). MPAs with continued fishing activities within Eastern Rockall correspond to locations where dives #7 and #8 took place. Dives #7 and #8 account for biotopes five and nine that possess vulnerable species *D. pertusum* and *M. oculata*. While the Rockall Escarpment is a steep environment providing a refuge for CWCs serving as important habitat-building species like *D. pertusum*, the uncertainty in the boundaries of these closures contributes to the inaccuracy of the term ‘refuge’ (Puerta et al., 2020). Understanding the location of these CWCs will help when protecting them from fisheries (Huvenne et al., 2016). However, climate change has provided additional threats to CWCs apart from past fishing activities. Limited existing management measures are monitoring disturbances due to climate change and unfortunately, area-based management, such as MPAs, will not protect CWCs against climate change (Johnson et al., 2019).

4.2 Importance of a biotope under climate change

Serving as fixed trackable units, biotopes contribute to the replicability of results obtained through distribution modelling (Gonzalez-Mirelis & Buhl-Mortensen, 2015). Biotopes can provide researchers with insight into the composition of conservation areas, such as MPAs and refuges, and can be further incorporated into marine spatial planning (Robinson et al., 2011). Baseline research has contributed to monitoring areas of significance and has allowed for the assessment of impacts of environmental stressors such as acidification and warming (Le et al., 2017). However, it is important to note the “looseness” with the term baseline, as data that is recorded and observed, is already data

that has changed over time. The efficacy and success of MPAs depend on the degree of consideration given to climate change in MPA design and management (Edgar et al., 2014; Tittensor et al., 2019). This opens the question of implementing climate adaptive management approaches, as a well-designed and managed MPA can be used as a mitigation and adaptation tool under a changing climate (Gormley et al., 2015). Understanding and coming to appreciate the variability in ecological conditions (natural variability), and ongoing climate change, is key to adaptive management (Levin et al., 2020). Unfortunately, one study represents but a snapshot in time and is not an adequate capture of natural variability.

5. **Conclusion**

The Rockall Escarpment is complex in both its bathymetry and the species that inhabit it. This study can help inform further ecologically driven sampling efforts off Rockall Bank by furthering our understanding of the vulnerable and indicative species present in the area. The abundance of *S. variabilis*, along with the vulnerable species *D. pertusum*, are important observations for the conservation and protection of this area. This study outlined the megafaunal biodiversity and the spatial variation of biotopes, and will serve as valuable baseline research within the Rockall Escarpment.

6. **References**

- Allcock, A. L., & Johnson, M. P. (2019). Interactions in the Deep Sea. In S. J. Hawkins, K. Bohn, L. B. Firth, & G. A. Williams (Eds.), *Interactions in the Marine Benthos* (1st ed., pp. 474–487). Cambridge University Press. <https://doi.org/10.1017/9781108235792.020>

- Arlinghaus, P., Zhang, W., Wrede, A., Schrum, C., & Neumann, A. (2021). Impact of benthos on morphodynamics from a modelling perspective. *Earth-Science Reviews*, 221, 103803. <https://doi.org/10.1016/j.earscirev.2021.103803>
- Arndt, D. S., Baringer, M. O., & Johnson, M. R. (2010). State of the Climate in 2009. *Bulletin of the American Meteorological Society*, 91(7), s1–s222. <https://doi.org/10.1175/BAMS-91-7-StateoftheClimate>
- Arya, D. B., Vincent, S. G. T., & Godson, P. S. (2022). Benthic biotopes: Abiotic and biotic factors in the sediment. In *Ecology and Biodiversity of Benthos* (pp. 21–31). Elsevier. <https://doi.org/10.1016/B978-0-12-821161-8.00009-X>
- Beaumont, N. J., Austen, M. C., Atkins, J. P., Burdon, D., Degraer, S., Dentinho, T. P., Deros, S., Holm, P., Horton, T., van Ierland, E., Marboe, A. H., Starkey, D. J., Townsend, M., & Zarzycki, T. (2007). Identification, definition and quantification of goods and services provided by marine biodiversity: Implications for the ecosystem approach. *Marine Pollution Bulletin*, 54(3), 253–265. <https://doi.org/10.1016/j.marpolbul.2006.12.003>
- Bonneau, L., Colin, C., Pons-Branchu, E., Mienis, F., Tisnérat-Laborde, N., Blamart, D., Elliot, M., Collart, T., Frank, N., Foliot, L., & Douville, E. (2018). Imprint of Holocene Climate Variability on Cold-Water Coral Reef Growth at the SW Rockall Trough Margin, NE Atlantic. *Geochemistry, Geophysics, Geosystems*, 19(8), 2437–2452. <https://doi.org/10.1029/2018GC007502>
- Borcard, D., Gillet, F., & Legendre, P. (2011). *Numerical Ecology with R*. Springer New York. <https://doi.org/10.1007/978-1-4419-7976-6>
- Brown, C. J., Smith, S. J., Lawton, P., & Anderson, J. T. (2011). Benthic habitat mapping: A review of progress towards improved understanding of the spatial ecology of the

- seafloor using acoustic techniques. *Estuarine, Coastal and Shelf Science*, 92(3), 502–520. <https://doi.org/10.1016/j.ecss.2011.02.007>
- Büscher, J. V., Form, A. U., & Riebesell, U. (2017). Interactive Effects of Ocean Acidification and Warming on Growth, Fitness and Survival of the Cold-Water Coral *Lophelia pertusa* under Different Food Availabilities. *Frontiers in Marine Science*, 4, 101. <https://doi.org/10.3389/fmars.2017.00101>
- Culwick, T., Phillips, J., Goodwin, C., Rayfield, E. J., & Hendry, K. R. (2020). Sponge Density and Distribution Constrained by Fluid Forcing in the Deep Sea. *Frontiers in Marine Science*, 7, 395. <https://doi.org/10.3389/fmars.2020.00395>
- Davies, A. J., & Guinotte, J. M. (2011). Global Habitat Suitability for Framework-Forming Cold-Water Corals. *PLoS ONE*, 6(4), e18483. <https://doi.org/10.1371/journal.pone.0018483>
- Davies, J. S., Stewart, H. A., Narayanaswamy, B. E., Jacobs, C., Spicer, J., Golding, N., & Howell, K. L. (2015). Benthic Assemblages of the Anton Dohrn Seamount (NE Atlantic): Defining Deep-Sea Biotopes to Support Habitat Mapping and Management Efforts with a Focus on Vulnerable Marine Ecosystems. *PLOS ONE*, 10(5), e0124815. <https://doi.org/10.1371/journal.pone.0124815>
- Dimitrakopoulos, P. G., & Troumbis, A. Y. (2019). Biotopes. In *Encyclopedia of Ecology* (pp. 359–365). Elsevier. <https://doi.org/10.1016/B978-0-12-409548-9.10923-6>
- Dufrêne, M., & Legendre, P. (1997). SPECIES ASSEMBLAGES AND INDICATOR SPECIES: THE NEED FOR A FLEXIBLE ASYMMETRICAL APPROACH. *Ecological Monographs*, 67(3), 345–366. [https://doi.org/10.1890/0012-9615\(1997\)067\[0345:SAAIST\]2.0.CO;2](https://doi.org/10.1890/0012-9615(1997)067[0345:SAAIST]2.0.CO;2)

- Edgar, G. J., Stuart-Smith, R. D., Willis, T. J., Kininmonth, S., Baker, S. C., Banks, S., Barrett, N. S., Becerro, M. A., Bernard, A. T. F., Berkhout, J., Buxton, C. D., Campbell, S. J., Cooper, A. T., Davey, M., Edgar, S. C., Försterra, G., Galván, D. E., Irigoyen, A. J., Kushner, D. J., ... Thomson, R. J. (2014). Global conservation outcomes depend on marine protected areas with five key features. *Nature*, *506*(7487), 216–220.
<https://doi.org/10.1038/nature13022>
- Fosså, J. H., Mortensen, P. B., & Furevik, D. M. (2002). The deep-water coral *Lophelia pertusa* in Norwegian waters: Distribution and fishery impacts. *Hydrobiologia*, *471*(1/3), 1–12.
<https://doi.org/10.1023/A:1016504430684>
- Gage, J. D. (1986). The benthic fauna of the Rockall Trough: Regional distribution and bathymetric zonation. *Proceedings of the Royal Society of Edinburgh. Section B. Biological Sciences*, *88*, 159–174. <https://doi.org/10.1017/S026972700000453X>
- Gammon, M. J., Tracey, D. M., Marriott, P. M., Cummings, V. J., & Davy, S. K. (2018). The physiological response of the deep-sea coral *Solenosmilia variabilis* to ocean acidification. *PeerJ*, *6*, e5236. <https://doi.org/10.7717/peerj.5236>
- GEBCO Bathymetric Compilation Group 2022. (2022). *The GEBCO_2022 Grid—A continuous terrain model of the global oceans and land*. (Version 1) [Documents, Network Common Data Form]. NERC EDS British Oceanographic Data Centre NOC.
<https://doi.org/10.5285/E0F0BB80-AB44-2739-E053-6C86ABC0289C>
- Georgiopolou, A., Shannon, P. M., Sacchetti, F., Haughton, P. D. W., & Benetti, S. (2013). Basement-controlled multiple slope collapses, Rockall Bank Slide Complex, NE Atlantic. *Marine Geology*, *336*, 198–214. <https://doi.org/10.1016/j.margeo.2012.12.003>

- Gonzalez-Mirelis, G., & Buhl-Mortensen, P. (2015). Modelling benthic habitats and biotopes off the coast of Norway to support spatial management. *Ecological Informatics*, 30, 284–292. <https://doi.org/10.1016/j.ecoinf.2015.06.005>
- Gormley, K. S. G., Hull, A. D., Porter, J. S., Bell, M. C., & Sanderson, W. G. (2015). Adaptive management, international co-operation and planning for marine conservation hotspots in a changing climate. *Marine Policy*, 53, 54–66. <https://doi.org/10.1016/j.marpol.2014.11.017>
- Griffiths, J. R., Kadin, M., Nascimento, F. J. A., Tamelander, T., Törnroos, A., Bonaglia, S., Bonsdorff, E., Brüchert, V., Gårdmark, A., Järnström, M., Kotta, J., Lindegren, M., Nordström, M. C., Norkko, A., Olsson, J., Weigel, B., Žydelis, R., Blenckner, T., Niiranen, S., & Winder, M. (2017). The importance of benthic-pelagic coupling for marine ecosystem functioning in a changing world. *Global Change Biology*, 23(6), 2179–2196. <https://doi.org/10.1111/gcb.13642>
- Harvey, J. (1982). θ -S relationships and water masses in the eastern North Atlantic. *Deep Sea Research Part A. Oceanographic Research Papers*, 29(8), 1021–1033. [https://doi.org/10.1016/0198-0149\(82\)90025-5](https://doi.org/10.1016/0198-0149(82)90025-5)
- Hebbeln, D., Portilho-Ramos, R. da C., Wienberg, C., & Titschack, J. (2019). The Fate of Cold-Water Corals in a Changing World: A Geological Perspective. *Frontiers in Marine Science*, 6, 119. <https://doi.org/10.3389/fmars.2019.00119>
- Hebbeln, D., Wienberg, C., Dullo, W.-C., Freiwald, A., Mienis, F., Orejas, C., & Titschack, J. (2020). Cold-water coral reefs thriving under hypoxia. *Coral Reefs*, 39(4), 853–859. <https://doi.org/10.1007/s00338-020-01934-6>

- Helm, K. P., Bindoff, N. L., & Church, J. A. (2011). Observed decreases in oxygen content of the global ocean: GLOBAL DECREASES IN OCEAN OXYGEN LEVELS. *Geophysical Research Letters*, 38(23), n/a-n/a. <https://doi.org/10.1029/2011GL049513>
- Hennige, S. J., Wicks, L. C., Kamenos, N. A., Perna, G., Findlay, H. S., & Roberts, J. M. (2015). Hidden impacts of ocean acidification to live and dead coral framework. *Proceedings of the Royal Society B: Biological Sciences*, 282(1813), 20150990. <https://doi.org/10.1098/rspb.2015.0990>
- Howe, J. A., Stoker, M. S., Masson, D. G., Pudsey, C. J., Morris, P., Larter, R. D., & Bulat, J. (2006). Seabed morphology and the bottom-current pathways around Rosemary Bank seamount, northern Rockall Trough, North Atlantic. *Marine and Petroleum Geology*, 23(2), 165–181. <https://doi.org/10.1016/j.marpetgeo.2005.08.003>
- Howell, K. L. (2010). A benthic classification system to aid in the implementation of marine protected area networks in the deep/high seas of the NE Atlantic. *Biological Conservation*, 143(5), 1041–1056. <https://doi.org/10.1016/j.biocon.2010.02.001>
- Huthnance, J. M. (1986). The Rockall slope current and shelf-edge processes. *Proceedings of the Royal Society of Edinburgh. Section B. Biological Sciences*, 88, 83–101. <https://doi.org/10.1017/S0269727000004486>
- Huvenne, V. A. I., Bett, B. J., Masson, D. G., Le Bas, T. P., & Wheeler, A. J. (2016). Effectiveness of a deep-sea cold-water coral Marine Protected Area, following eight years of fisheries closure. *Biological Conservation*, 200, 60–69. <https://doi.org/10.1016/j.biocon.2016.05.030>

- Johnson, D., Adelaide Ferreira, M., & Kenchington, E. (2018). Climate change is likely to severely limit the effectiveness of deep-sea ABMTs in the North Atlantic. *Marine Policy*, 87, 111–122. <https://doi.org/10.1016/j.marpol.2017.09.034>
- Johnson, D. E., Barrio Froján, C., Neat, F., Van Oevelen, D., Stirling, D., Gubbins, M. J., & Roberts, J. M. (2019). Rockall and Hatton: Resolving a Super Wicked Marine Governance Problem in the High Seas of the Northeast Atlantic Ocean. *Frontiers in Marine Science*, 6, 69. <https://doi.org/10.3389/fmars.2019.00069>
- Jones, C. G., Gutiérrez, J. L., Byers, J. E., Crooks, J. A., Lambrinos, J. G., & Talley, T. S. (2010). A framework for understanding physical ecosystem engineering by organisms. *Oikos*, 119(12), 1862–1869. <https://doi.org/10.1111/j.1600-0706.2010.18782.x>
- Jones, C. G., Lawton, J. H., & Shachak, M. (1994). Organisms as Ecosystem Engineers. *Oikos*, 69(3), 373. <https://doi.org/10.2307/3545850>
- Jones, C. G., Lawton, J. H., & Shachak, M. (1997). POSITIVE AND NEGATIVE EFFECTS OF ORGANISMS AS PHYSICAL ECOSYSTEM ENGINEERS. *Ecology*, 78(7), 1946–1957. [https://doi.org/10.1890/0012-9658\(1997\)078\[1946:PANEOO\]2.0.CO;2](https://doi.org/10.1890/0012-9658(1997)078[1946:PANEOO]2.0.CO;2)
- Kerry, R. G., Montalbo, F. J. P., Das, R., Patra, S., Mahapatra, G. P., Maurya, G. K., Nayak, V., Jena, A. B., Ukhurebor, K. E., Jena, R. C., Gouda, S., Majhi, S., & Rout, J. R. (2022). An overview of remote monitoring methods in biodiversity conservation. *Environmental Science and Pollution Research*, 29(53), 80179–80221. <https://doi.org/10.1007/s11356-022-23242-y>
- Kremen, C. (2005). Managing ecosystem services: What do we need to know about their ecology?: Ecology of ecosystem services. *Ecology Letters*, 8(5), 468–479. <https://doi.org/10.1111/j.1461-0248.2005.00751.x>

- Kristensen, E., Penha-Lopes, G., Delefosse, M., Valdemarsen, T., Quintana, C., & Banta, G. (2012). What is bioturbation? The need for a precise definition for fauna in aquatic sciences. *Marine Ecology Progress Series*, 446, 285–302. <https://doi.org/10.3354/meps09506>
- Le, J. T., Levin, L. A., & Carson, R. T. (2017). Incorporating ecosystem services into environmental management of deep-seabed mining. *Deep Sea Research Part II: Topical Studies in Oceanography*, 137, 486–503. <https://doi.org/10.1016/j.dsr2.2016.08.007>
- Legendre, P., & Borcard, D. (2018). Box-Cox-chord transformations for community composition data prior to beta diversity analysis. *Ecography*, 41(11), 1820–1824. <https://doi.org/10.1111/ecog.03498>
- Levin, L. A., Bett, B. J., Gates, A. R., Heimbach, P., Howe, B. M., Janssen, F., McCurdy, A., Ruhl, H. A., Snelgrove, P., Stocks, K. I., Bailey, D., Baumann-Pickering, S., Beaverson, C., Benfield, M. C., Booth, D. J., Carreiro-Silva, M., Colaço, A., Eblé, M. C., Fowler, A. M., ... Weller, R. A. (2019). Global Observing Needs in the Deep Ocean. *Frontiers in Marine Science*, 6, 241. <https://doi.org/10.3389/fmars.2019.00241>
- Levin, L. A., Wei, C., Dunn, D. C., Amon, D. J., Ashford, O. S., Cheung, W. W. L., Colaço, A., Dominguez-Carrió, C., Escobar, E. G., Harden-Davies, H. R., Drazen, J. C., Ismail, K., Jones, D. O. B., Johnson, D. E., Le, J. T., Lejzerowicz, F., Mitarai, S., Morato, T., Mulsow, S., ... Yasuhara, M. (2020). Climate change considerations are fundamental to management of deep-sea resource extraction. *Global Change Biology*, 26(9), 4664–4678. <https://doi.org/10.1111/gcb.15223>
- Levin, L. A., Whitcraft, C. R., Mendoza, G. F., Gonzalez, J. P., & Cowie, G. (2009). Oxygen and organic matter thresholds for benthic faunal activity on the Pakistan margin oxygen

- minimum zone (700–1100m). *Deep Sea Research Part II: Topical Studies in Oceanography*, 56(6–7), 449–471. <https://doi.org/10.1016/j.dsr2.2008.05.032>
- Levin, S. A., & Lubchenco, J. (2008). Resilience, Robustness, and Marine Ecosystem-based Management. *BioScience*, 58(1), 27–32. <https://doi.org/10.1641/B580107>
- Leys, S. P., & Meech, R. W. (2006). Physiology of coordination in sponges. *Canadian Journal of Zoology*, 84(2), 288–306. <https://doi.org/10.1139/z05-171>
- Lohrer, A. M., Thrush, S. F., & Gibbs, M. M. (2004). Bioturbators enhance ecosystem function through complex biogeochemical interactions. *Nature*, 431(7012), 1092–1095. <https://doi.org/10.1038/nature03042>
- Mermillod-Blondin, F., & Rosenberg, R. (2006). Ecosystem engineering: The impact of bioturbation on biogeochemical processes in marine and freshwater benthic habitats. *Aquatic Sciences*, 68(4), 434–442. <https://doi.org/10.1007/s00027-006-0858-x>
- Mienis, F., de Stigter, H. C., de Haas, H., & van Weering, T. C. E. (2009). Near-bed particle deposition and resuspension in a cold-water coral mound area at the Southwest Rockall Trough margin, NE Atlantic. *Deep Sea Research Part I: Oceanographic Research Papers*, 56(6), 1026–1038. <https://doi.org/10.1016/j.dsr.2009.01.006>
- Morato, T., González-Irusta, J., Dominguez-Carrió, C., Wei, C., Davies, A., Sweetman, A. K., Taranto, G. H., Beazley, L., García-Alegre, A., Grehan, A., Laffargue, P., Murillo, F. J., Sacau, M., Vaz, S., Kenchington, E., Arnaud-Haond, S., Callery, O., Chimienti, G., Cordes, E., ... Carreiro-Silva, M. (2020). Climate-induced changes in the suitable habitat of cold-water corals and commercially important deep-sea fishes in the North Atlantic. *Global Change Biology*, 26(4), 2181–2202. <https://doi.org/10.1111/gcb.14996>

- Mortensen, P. B., Buhl-Mortensen, L., Gebruk, A. V., & Krylova, E. M. (2008). Occurrence of deep-water corals on the Mid-Atlantic Ridge based on MAR-ECO data. *Deep Sea Research Part II: Topical Studies in Oceanography*, 55(1–2), 142–152. <https://doi.org/10.1016/j.dsr2.2007.09.018>
- Murtagh, F. (1984). Counting dendrograms: A survey. *Discrete Applied Mathematics*, 7(2), 191–199. [https://doi.org/10.1016/0166-218X\(84\)90066-0](https://doi.org/10.1016/0166-218X(84)90066-0)
- Naidoo, R., Balmford, A., Costanza, R., Fisher, B., Green, R. E., Lehner, B., Malcolm, T. R., & Ricketts, T. H. (2008). Global mapping of ecosystem services and conservation priorities. *Proceedings of the National Academy of Sciences*, 105(28), 9495–9500. <https://doi.org/10.1073/pnas.0707823105>
- New, A. L., & Smythe-Wright, D. (2001). Aspects of the circulation in the Rockall Trough. *Continental Shelf Research*, 21(8–10), 777–810. [https://doi.org/10.1016/S0278-4343\(00\)00113-8](https://doi.org/10.1016/S0278-4343(00)00113-8)
- Oevelen, D. van, Duineveld, G., Lavaleye, M., Mienis, F., Soetaert, K., & Heip, C. H. R. (2009). The cold-water coral community as hotspot of carbon cycling on continental margins: A food-web analysis from Rockall Bank (northeast Atlantic). *Limnology and Oceanography*, 54(6), 1829–1844. <https://doi.org/10.4319/lo.2009.54.6.1829>
- Pawlik, J. R., & McMurray, S. E. (2020). The Emerging Ecological and Biogeochemical Importance of Sponges on Coral Reefs. *Annual Review of Marine Science*, 12(1), 315–337. <https://doi.org/10.1146/annurev-marine-010419-010807>
- Penny Holliday, N., Pollard, R. T., Read, J. F., & Leach, H. (2000). Water mass properties and fluxes in the Rockall Trough, 1975–1998. *Deep Sea Research Part I: Oceanographic Research Papers*, 47(7), 1303–1332. [https://doi.org/10.1016/S0967-0637\(99\)00109-0](https://doi.org/10.1016/S0967-0637(99)00109-0)

- Piechaud, N., Downie, A., Stewart, H. A., & Howell, K. L. (2014). The impact of modelling method selection on predicted extent and distribution of deep-sea benthic assemblages. *Earth and Environmental Science Transactions of the Royal Society of Edinburgh*, *105*(4), 251–261. <https://doi.org/10.1017/S1755691015000122>
- Pinsky, M. L., Selden, R. L., & Kitchel, Z. J. (2020). Climate-Driven Shifts in Marine Species Ranges: Scaling from Organisms to Communities. *Annual Review of Marine Science*, *12*(1), 153–179. <https://doi.org/10.1146/annurev-marine-010419-010916>
- Price, D. M., Robert, K., Callaway, A., Lo lacono, C., Hall, R. A., & Huvenne, V. A. I. (2019). Using 3D photogrammetry from ROV video to quantify cold-water coral reef structural complexity and investigate its influence on biodiversity and community assemblage. *Coral Reefs*, *38*(5), 1007–1021. <https://doi.org/10.1007/s00338-019-01827-3>
- Przeslawski, R., Ahyong, S., Byrne, M., Wörheide, G., & Hutchings, P. (2008). Beyond corals and fish: The effects of climate change on noncoral benthic invertebrates of tropical reefs: TROPICAL BENTHIC INVERTEBRATES AND CLIMATE CHANGE. *Global Change Biology*, *14*(12), 2773–2795. <https://doi.org/10.1111/j.1365-2486.2008.01693.x>
- Puerta, P., Johnson, C., Carreiro-Silva, M., Henry, L.-A., Kenchington, E., Morato, T., Kazanidis, G., Rueda, J. L., Urra, J., Ross, S., Wei, C.-L., González-Irusta, J. M., Arnaud-Haond, S., & Orejas, C. (2020). Influence of Water Masses on the Biodiversity and Biogeography of Deep-Sea Benthic Ecosystems in the North Atlantic. *Frontiers in Marine Science*, *7*, 239. <https://doi.org/10.3389/fmars.2020.00239>
- Pusceddu, A., Carugati, L., Gambi, C., Mienert, J., Petani, B., Sanchez-Vidal, A., Canals, M., Heussner, S., & Danovaro, R. (2016). Organic matter pools, C turnover and meiofaunal biodiversity in the sediments of the western Spitsbergen deep continental margin,

- Svalbard Archipelago. *Deep Sea Research Part I: Oceanographic Research Papers*, 107, 48–58. <https://doi.org/10.1016/j.dsr.2015.11.004>
- Read, J. F. (2000). CONVEX-91: Water masses and circulation of the Northeast Atlantic subpolar gyre. *Progress in Oceanography*, 48(4), 461–510. [https://doi.org/10.1016/S0079-6611\(01\)00011-8](https://doi.org/10.1016/S0079-6611(01)00011-8)
- Robert, K., Jones, D., & Huvenne, V. (2014). Megafaunal distribution and biodiversity in a heterogeneous landscape: The iceberg-scoured Rockall Bank, NE Atlantic. *Marine Ecology Progress Series*, 501, 67–88. <https://doi.org/10.3354/meps10677>
- Roberts, C. (2002). Deep impact: The rising toll of fishing in the deep sea. *Trends in Ecology & Evolution*, 17(5), 242–245. [https://doi.org/10.1016/S0169-5347\(02\)02492-8](https://doi.org/10.1016/S0169-5347(02)02492-8)
- Roberts, J. M., Henry, L.-A., Long, D., & Hartley, J. P. (2008). Cold-water coral reef frameworks, megafaunal communities and evidence for coral carbonate mounds on the Hatton Bank, north east Atlantic. *Facies*, 54(3), 297–316. <https://doi.org/10.1007/s10347-008-0140-x>
- Robinson, K. A., Ramsay, K., Lindenbaum, C., Frost, N., Moore, J., Wright, A. P., & Petrey, D. (2011). Predicting the distribution of seabed biotopes in the southern Irish Sea. *Continental Shelf Research*, 31(2), S120–S131. <https://doi.org/10.1016/j.csr.2010.01.010>
- Rogers, A. D. (1999). The Biology of *Lophelia pertusa* (L innaeus 1758) and Other Deep-Water Reef-Forming Corals and Impacts from Human Activities. *International Review of Hydrobiology*, 84(4), 315–406. <https://doi.org/10.1002/iroh.199900032>
- Romero, G. Q., Gonçalves-Souza, T., Vieira, C., & Koricheva, J. (2015). Ecosystem engineering effects on species diversity across ecosystems: A meta-analysis: Ecosystem

engineering effects across ecosystems. *Biological Reviews*, 90(3), 877–890.

<https://doi.org/10.1111/brv.12138>

Samuelsen, A., Schrum, C., Yumruktepe, V. Ç., Daewel, U., & Roberts, E. M. (2022).

Environmental Change at Deep-Sea Sponge Habitats Over the Last Half Century: A Model Hindcast Study for the Age of Anthropogenic Climate Change. *Frontiers in Marine Science*, 9, 737164. <https://doi.org/10.3389/fmars.2022.737164>

Schoening, T., Osterloff, J., & Nattkemper, T. W. (2016). RecoMIA—Recommendations for

Marine Image Annotation: Lessons Learned and Future Directions. *Frontiers in Marine Science*, 3. <https://doi.org/10.3389/fmars.2016.00059>

Seitz, R. D., Wennhage, H., Bergström, U., Lipcius, R. N., & Ysebaert, T. (2014). Ecological

value of coastal habitats for commercially and ecologically important species. *ICES Journal of Marine Science*, 71(3), 648–665. <https://doi.org/10.1093/icesjms/fst152>

Selig, E. R., Hole, D. G., Allison, E. H., Arkema, K. K., McKinnon, M. C., Chu, J., Sherbinin,

A., Fisher, B., Glew, L., Holland, M. B., Ingram, J. C., Rao, N. S., Russell, R. B.,

Srebotnjak, T., Teh, L. C. L., Troëng, S., Turner, W. R., & Zvoleff, A. (2019). Mapping global human dependence on marine ecosystems. *Conservation Letters*, 12(2).

<https://doi.org/10.1111/conl.12617>

Smith, C. R., A. Levin, L., Hoover, D. J., McMurtry, G., & Gage, J. D. (2000). Variations in

bioturbation across the oxygen minimum zone in the northwest Arabian Sea. *Deep Sea Research Part II: Topical Studies in Oceanography*, 47(1–2), 227–257.

[https://doi.org/10.1016/S0967-0645\(99\)00108-3](https://doi.org/10.1016/S0967-0645(99)00108-3)

Smith C. R., Pope R. H., DeMaster D. J., Magaard L.. Age-dependent mixing of deep-sea sediments, *Geochimica et Cosmochimica Acta*, 1993, vol. 57 (pg. 1473-1488)

[10.1016/0016-7037\(93\)90007-J](https://doi.org/10.1016/0016-7037(93)90007-J)

- Smith, C. R., Berelson, W., Demaster, D. J., Dobbs, F. C., Hammond, D., Hoover, D. J., Pope, R. H., & Stephens, M. (1997). Latitudinal variations in benthic processes in the abyssal equatorial Pacific: Control by biogenic particle flux. *Deep Sea Research Part II: Topical Studies in Oceanography*, 44(9–10), 2295–2317. [https://doi.org/10.1016/S0967-0645\(97\)00022-2](https://doi.org/10.1016/S0967-0645(97)00022-2)
- Solan, M., Cardinale, B. J., Downing, A. L., Engelhardt, K. A. M., Ruesink, J. L., & Srivastava, D. S. (2004). Extinction and Ecosystem Function in the Marine Benthos. *Science*, 306(5699), 1177–1180. <https://doi.org/10.1126/science.1103960>
- Solomon, S., Intergovernmental Panel on Climate Change, & Intergovernmental Panel on Climate Change (Eds.). (2007). *Climate change 2007: The physical science basis: contribution of Working Group I to the Fourth Assessment Report of the Intergovernmental Panel on Climate Change*. Cambridge University Press.
- Stevens, T., & Connolly, R. M. (2004). Testing the utility of abiotic surrogates for marine habitat mapping at scales relevant to management. *Biological Conservation*, 119(3), 351–362. <https://doi.org/10.1016/j.biocon.2003.12.001>
- Sweetman, A. K., Thurber, A. R., Smith, C. R., Levin, L. A., Mora, C., Wei, C.-L., Gooday, A. J., Jones, D. O. B., Rex, M., Yasuhara, M., Ingels, J., Ruhl, H. A., Frieder, C. A., Danovaro, R., Würzberg, L., Baco, A., Grupe, B. M., Pasulka, A., Meyer, K. S., ... Roberts, J. M. (2017). Major impacts of climate change on deep-sea benthic ecosystems. *Elementa: Science of the Anthropocene*, 5, 4. <https://doi.org/10.1525/elementa.203>
- Tittensor, D. P., Beger, M., Boerder, K., Boyce, D. G., Cavanagh, R. D., Cosandey-Godin, A., Crespo, G. O., Dunn, D. C., Ghiffary, W., Grant, S. M., Hannah, L., Halpin, P. N.,

- Harfoot, M., Heaslip, S. G., Jeffery, N. W., Kingston, N., Lotze, H. K., McGowan, J., McLeod, E., ... Worm, B. (2019). Integrating climate adaptation and biodiversity conservation in the global ocean. *Science Advances*, 5(11), eaay9969.
<https://doi.org/10.1126/sciadv.aay9969>
- Tittensor, D. P., Rex, M. A., Stuart, C. T., McClain, C. R., & Smith, C. R. (2011). Species–energy relationships in deep-sea molluscs. *Biology Letters*, 7(5), 718–722.
<https://doi.org/10.1098/rsbl.2010.1174>
- Weaver, P., & Johnson, D. (2012). Think big for marine conservation. *Nature*, 483(7390), 399–399. <https://doi.org/10.1038/483399a>
- Weinert, M., Kröncke, I., Meyer, J., Mathis, M., Pohlmann, T., & Reiss, H. (2022). Benthic ecosystem functioning under climate change: Modelling the bioturbation potential for benthic key species in the southern North Sea. *PeerJ*, 10, e14105.
<https://doi.org/10.7717/peerj.14105>
- Wienberg, C., Beuck, L., Heidkamp, S., Hebbeln, D., Freiwald, A., Pfannkuche, O., & Monteys, X. (2008). Franken Mound: Facies and biocoenoses on a newly-discovered “carbonate mound” on the western Rockall Bank, NE Atlantic. *Facies*, 54(1), 1–24.
<https://doi.org/10.1007/s10347-007-0118-0>
- Wilson, J. B. (1979a). ‘Patch’ development of the deep-water coral *Lophelia Pertusa* (L.) on Rockall Bank. *Journal of the Marine Biological Association of the United Kingdom*, 59(1), 165–177. <https://doi.org/10.1017/S0025315400046257>
- Wilson, J. B. (1979b). The distribution of the coral *Lophelia pertusa* (L.) [*L. prolifera* (Pallas)] in the north-east Atlantic. *Journal of the Marine Biological Association of the United Kingdom*, 59(1), 149–164. <https://doi.org/10.1017/S0025315400046245>

- Woolley, S. N. C., Tittensor, D. P., Dunstan, P. K., Guillera-Arroita, G., Lahoz-Monfort, J. J., Wintle, B. A., Worm, B., & O'Hara, T. D. (2016). Deep-sea diversity patterns are shaped by energy availability. *Nature*, *533*(7603), 393–396.
<https://doi.org/10.1038/nature17937>
- Wrede, A., Dannheim, J., Gutow, L., & Brey, T. (2017). Who really matters: Influence of German Bight key bioturbators on biogeochemical cycling and sediment turnover. *Journal of Experimental Marine Biology and Ecology*, *488*, 92–101.
<https://doi.org/10.1016/j.jembe.2017.01.001>
- Wright, J. P., Gurney, W. S. C., & Jones, C. G. (2004). Patch dynamics in a landscape modified by ecosystem engineers. *Oikos*, *105*(2), 336–348. <https://doi.org/10.1111/j.003>

7. Appendices

7.1 Species ID for all discriminating species assigned from SIMPER and IndVal

Morphospecies label	Phylum	Subphylum	Class	Subclass	Order	Suborder	Family	Genus	Species	Morphospecies ID
ASC1	Chordata	Tunicata	Asciacea	NA	NA	NA	NA	NA	NA	Asciacea species 1
CHAC	Arthropoda	Crustacea	Malacostraca	Eumalacostraca	Decapoda	Pleocyemata	Geryonidae	Chaceon	NA	Chaceon species 1
MAJ1	Arthropoda	Crustacea	Malacostraca	Eumalacostraca	Decapoda	NA	NA	NA	NA	Decapoda
SHRMP	Arthropoda	Crustacea	Malacostraca	Eumalacostraca	Decapoda	NA	NA	NA	NA	Shrimp species
WSQUAT	Arthropoda	Crustacea	Malacostraca	Eumalacostraca	Decapoda	Pleocyemata	NA	NA	NA	Galatheaidea
RET	Bryozoa	NA	Gymnolaemata	NA	Cheilostomatida	Flustrina	Phidoloporidae	Reteporella	NA	Reteporella
EPIZOA	Cnidaria	NA	Anthozoa	Hexacorallia	Zoantharia	Macrocnemina	Epizoanthidae	Epizoanthus	<i>Epizoanthus paguriphilus</i>	<i>Epizoanthus paguriphilus</i>
SCORA19	Cnidaria	NA	Anthozoa	Hexacorallia	Scleractinia	NA	Flabellidae	NA	NA	Flabellidae
SCORA2	Cnidaria	NA	Anthozoa	Hexacorallia	Scleractinia	NA	Flabellidae	Flabellum	Flabellum alabastrum	Flabellum alabastrum
VNUS2	Cnidaria	NA	Anthozoa	Hexacorallia	Actiniaria	Enthemonae	Actinoscyphiidae	Actinoscyphia	NA	Actinoscyphia
CALLO	Cnidaria	NA	Anthozoa	Octocorallia	Scleralecyonacea		Primnoidae	Callogorgia	NA	Callogorgia species 1
LEIO	Cnidaria	NA	Anthozoa	Hexacorallia	Antipatharia	NA	NA	Leiopathes	NA	Leiopathes species
LOPH	Cnidaria	NA	Anthozoa	Hexacorallia	Scleractinia	NA	Caryophylliidae	Desmophyllum	<i>Desmophyllum pertusum</i>	<i>Desmophyllum pertusum</i>
MAD	Cnidaria	NA	Anthozoa	Hexacorallia	Scleractinia	NA	Oculinidae	Madrepora	<i>Madrepora oculata</i>	<i>Madrepora oculata</i>
PARA	Cnidaria	NA	Anthozoa	Octocorallia	Scleralecyonacea	NA	Coralliidae	<i>Parastichopus</i>	NA	<i>Parastichopus</i> sp.
PEN2	Cnidaria	NA	Anthozoa	Hexacorallia	Antipatharia	NA	Schizopathidae	Parantipathes	NA	Parantipathes
SOLE	Cnidaria	NA	Anthozoa	Hexacorallia	Scleractinia	NA	Caryophylliidae	Solenosmilia	<i>Solenosmilia variabilis</i>	<i>Solenosmilia variabilis</i>
CERI	Cnidaria	NA	Anthozoa	Ceriantharia	NA	NA	NA	NA	NA	Cerianthidae species 1
CNI1	Cnidaria	NA	Anthozoa	Hexacorallia	Actiniaria	NA	NA	NA	NA	Anthozoa species 1

CNI12	Cnidaria	NA	Anthozoa	Hexacorallia	Actiniaria	NA	NA	NA	NA	Anthozoa species 12
CNI14	Cnidaria	NA	Anthozoa	Hexacorallia	Scleractinia	NA	Flabellidae	Javania	NA	Anthozoa species 14
CNI4	Cnidaria	NA	Anthozoa	Hexacorallia	Actiniaria	NA	NA	NA	NA	Anthozoa species 4
CNI5	Cnidaria	NA	Anthozoa	Hexacorallia	Actiniaria	NA	NA	NA	NA	Anthozoa species 5
CNI6	Cnidaria	NA	Anthozoa	Hexacorallia	Actiniaria	Enthemonae	Actinostolidae	NA	NA	Anthozoa species 6
CNI8	Cnidaria	NA	Anthozoa	Hexacorallia	Actiniaria	Enthemonae	Actinostolidae	NA	NA	Anthozoa species 8
CNI9	Cnidaria	NA	Anthozoa	Hexacorallia	Actiniaria	Enthemonae	Actinostolidae	NA	NA	Anthozoa species 9
POMP	Cnidaria	NA	Anthozoa	Hexacorallia	Actiniaria	Enthemonae	Liponematidae	Liponema	<i>Liponema brevicome</i>	<i>Liponema brevicome</i>
PENTA	Echinodermata	Crinozoa	Crinoidea	Articulata	Comatulida		Pentametrocrinidae	Pentametrocrinus	NA	Pentametrocrinus
STAR7	Echinodermata	Asterozoa	Asteroidea	NA	NA	NA	NA	NA	NA	Asteroidea
BRIS1	Echinodermata	Asterozoa	Asteroidea	Ambuloasteroidea	Brisingida	NA	NA	NA	NA	Brisingida species 1
CALVE	Echinodermata	Echinozoa	Echinoidea	Euechinoidea	Echinothurioida	NA	Echinothuriidae	Calveriosoma	<i>Calveriosoma hystrix</i>	<i>Calveriosoma hystrix</i>
CID	Echinodermata	Echinozoa	Echinoidea	Cidaroida	Cidaroida	NA	Cidaridae	Cidaris	<i>Cidaris cidaris</i>	<i>Cidaris cidaris</i>
FSTAR1	Echinodermata	Crinozoa	Crinoidea	NA	NA	NA	NA	NA	NA	Crinoidea species 1
FSTAR2	Echinodermata	Crinozoa	Crinoidea	NA	NA	NA	NA	NA	NA	Crinoidea species 2
HOLO1	Echinodermata	Echinozoa	Holothuroidea	NA	NA	NA	NA	NA	NA	Holothuroidea species 1
HOLO3	Echinodermata	Echinozoa	Holothuroidea	NA	NA	NA	NA	NA	NA	Holothuroidea species 3
HOLO4	Echinodermata	Echinozoa	Holothuroidea	NA	NA	NA	NA	NA	NA	Holothuroidea species 4
OPHI1	Echinodermata	Asterozoa	Ophiuroidea	NA	NA	NA	NA	NA	NA	Ophiuroidea species 1
OPHI2	Echinodermata	Asterozoa	Ophiuroidea	NA	NA	NA	NA	NA	NA	Ophiuroidea species 2
OPHI3	Echinodermata	Asterozoa	Ophiuroidea	NA	NA	NA	NA	NA	NA	Ophiuroidea species 3
OPHI4	Echinodermata	Asterozoa	Ophiuroidea	NA	NA	NA	NA	NA	NA	Ophiuroidea species 4
URCH1	Echinodermata	Echinozoa	Echinoidea	Euechinoidea	Echinothurioida	NA	Echinothuriidae	NA	NA	Echinoidea species 1

URCH2	Echinodermata	Echinozoa	Echinoidea	Euechinoidea	Echinothurioida	NA	Echinothuriidae	NA	NA	Echinoidea species 2
URCH5	Echinodermata	Echinozoa	Echinoidea	Euechinoidea	Echinothurioida	NA	Echinothuriidae	Araeosoma	<i>Araeosoma fenestratum</i>	<i>Araeosoma fenestratum</i>
BOWL	Porifera	NA	Demospongiae	Heteroscleromorpha	Bubarida	NA	Bubaridae	Phakellia	NA	Phakellia species 1
FAN1	Porifera	NA	Demospongiae	Heteroscleromorpha	Bubarida	NA	Bubaridae	Phakellia	NA	Phakellia species 2
GSPNG	Porifera	NA	Demospongiae	NA	NA	NA	NA	NA	NA	Demospongiae
PORI10	Porifera	NA	Demospongiae	Heteroscleromorpha	Poecilosclerida	NA	Mycalidae	Mycale	NA	Porifera species 5
PORI11	Porifera	NA	Demospongiae	NA	NA	NA	NA	NA	NA	Porifera species 6
PORI3	Porifera	NA	Demospongiae	NA	NA	NA	NA	NA	NA	Porifera species 3
PORI8	Porifera	NA	Demospongiae	NA	NA	NA	NA	NA	NA	Porifera species 11
YSNG3	Porifera	NA	Demospongiae	Keratosa	Dendroceratida	NA	Darwinellidae	Aplysilla	<i>Aplysilla sulfurea</i>	<i>Aplysilla sulfurea</i>
YSPNG	Porifera	NA	Demospongiae	NA	NA	NA	NA	NA	NA	Demospongiae
EUPL2	Porifera	NA	Hexactinellida	Hexasterophora	Lyssacosida	NA	Rossellidae	Asconema	<i>Asconema foliatum</i>	<i>Asconema foliatum</i>

7.2 Results from the SIMPER analysis per biotope with the cumulative summary representing approximately 75% of the dissimilarity between the biotope pairs

Biotope 1 - 2			
Taxa	Biotope1 Average	Biotope 2 Average	Cumulative Summary
HOLO4	14.3333	0.5	0.617333
OPHI1	0	1.5	0.684862
OPHI3	0	1	0.729882
Biotope 1 - 3			
Taxa	Biotope 1 Average	Biotope 3 Average	Cumulative Summary
HOLO4	14.3333	0	0.494313
PARA	0	4	0.632465
HOLO1	0.33333	2.75	0.705157
Biotope 1 - 3			
Taxa	Biotope 1 Average	Biotope 4 Average	Cumulative Summary
CID	0.33333	34.37037	0.359952
HOLO4	14.3333	0.012346	0.615163
CERI	0.33333	31.2716	0.69841
Biotope 1 - 5			
Taxa	Biotope 1 Average	Biotope 5 Average	Cumulative Summary
GSPNG	0	59.16667	0.168399
CNI8	0	32.9697	0.335587
HOLO4	14.3333	0.227273	0.482507
MAD	0.33333	15.69697	0.558103
CNI14	0	8.787879	0.604197
BOWL	0	8.651515	0.641771
WSQUAT	0	6.863636	0.66756
RET	0	4.106061	0.688665
HOLO3	0	3.590909	0.709536
FAN1	0	4.121212	0.728333
CERI	0.33333	1.30303	0.746859
Biotope 1 - 6			
Taxa	Biotope 1 Average	Biotope 6 Average	Cumulative Summary
URCH5	0	296.2188	0.580979
Biotope 1 - 8			
Taxa	Biotope 1 Average	Biotope 8 Average	Cumulative Summary
URCH1	0	38.15556	0.330465
HOLO4	14.3333	0	0.642395
Biotope 1 - 9			
Taxa	Biotope 1 Average	Biotope 9 Average	Cumulative Summary
LOPH	0	73.3	0.466149

HOLO4	14.3333	0	0.596735
SCORA19	0	15.05	0.663313
STAR7	0	11.2	0.720127

Biotope 1 - 11

Taxa	Biotope 1 Average	Biotope 11 Average	Cumulative Summary
HOLO4	14.3333	0	0.440669
OPHI2	0	6.375	0.581593
CERI	0.33333	4.625	0.685285
CORALY2	0	1.375	0.721211
CNI5	1	0	0.750772

Biotope 1 - 12

Taxa	Biotope 1 Average	Biotope 12 Average	Cumulative Summary
CNI14	0	26.38596	0.109657
OPHI4	0	135.2807	0.213465
SOLE	0	47.61404	0.316064
PEN2	0	28.78947	0.410546
HOLO4	14.3333	0.017544	0.503744
EUPL2	0	25.35088	0.562455
YSPNG	0	18.4386	0.618477
CERI	0.33333	3.45614	0.647717
OPHI2	0	6.22807	0.676677
ASC1	0	7.684211	0.704785
PORI11	0	5.929825	0.729847
PORI8	0	5.859649	0.748524

Biotope 2 - 3

Taxa	Biotope 2 Average	Biotope 3 Average	Cumulative Summary
PARA	0.5	4	0.227392
OPHI1	1.5	0	0.329749
HOLO1	0	2.75	0.426896
CNI4	0	2.5	0.521253
OPHI3	1	0	0.589491
CALVE	0	1	0.650878
CARO	0	0.5	0.688559
CERI	0.5	0.25	0.722678

Biotope 2 - 4

Taxa	Biotope 2 Average	Biotope 4 Average	Cumulative Summary
CID	0.5	34.37037	0.472918
CERI	0.5	31.2716	0.568941
YSPNG	0	13.2963	0.632928
HOLO3	0	6.82716	0.681487
OPHI1	1.5	0	0.72277

Biotope 2 - 5

Taxa	Biotope 2 Average	Biotope 5 Average	Cumulative Summary
CNI8	0	32.9697	0.193479
GSPNG	0	59.16667	0.375076
MAD	0	15.69697	0.456628
CNI14	0	8.787879	0.510659
BOWL	0	8.651515	0.551294
WSQUAT	0	6.863636	0.579699
CERI	0.5	1.30303	0.60457
RET	0	4.106061	0.628322
HOLO3	0	3.590909	0.651502
OPHI1	1.5	0.19697	0.672623
FAN1	0	4.121212	0.693155
CNI6	0	3.272727	0.710119
CID	0.5	1.651515	0.725067
OPHI3	1	0.045455	0.739469
LEIO	0	3.469697	0.753611

Biotope 2 - 6

Taxa	Biotope 2 Average	Biotope 6 Average	Cumulative Summary
URCH5	0	296.2188	0.651802
OPHI1	1.5	0	0.684512
MAD	0	5.96875	0.713276
OPHI3	1	0.03125	0.735054
CID	0.5	2.5625	0.753988

Biotope 2 - 8

Taxa	Biotope 2 Average	Biotope 8 Average	Cumulative Summary
URCH1	0	38.15556	0.407939
CNI1	0	7.977778	0.595354
URCH2	0	3.644444	0.656755
OPHI1	1.5	0	0.707075
PAGU	0	1.444444	0.752015

Biotope 2 - 9

Taxa	Biotope 2 Average	Biotope 9 Average	Cumulative Summary
LOPH	0	73.3	0.528079
SCORA19	0	15.05	0.598777
STAR7	0	11.2	0.662212
LEIO	0	6.05	0.706158
MAJ1	0	3.7	0.731289
SCORA2	0	3.3	0.752999

Biotope 2 - 11

Taxa	Biotope 2 Average	Biotope 11 Average	Cumulative Summary
OPHI2	0	6.375	0.20731
CERI	0.5	4.625	0.362901

OPHI1	1.5	0	0.456672
OPHI3	1	0	0.519187
CORALY2	0	1.375	0.575392
OPHI4	0	0.875	0.616934
BSPNG	0	1.25	0.65183
CNI14	0	0.875	0.684689
PARA	0.5	0	0.715947
CID	0.5	0	0.747204

Biotope 2 - 12

Taxa	Biotope 2 Average	Biotope 12 Average	Cumulative Summary
CNI14	0	26.38596	0.123051
OPHI4	0	135.2807	0.230115
SOLE	0	47.61404	0.336992
PEN2	0	28.78947	0.438895
EUPL2	0	25.35088	0.502232
YSPNG	0	18.4386	0.563053
CERI	0.5	3.45614	0.596781
OPHI2	0	6.22807	0.629045
ASC1	0	7.684211	0.659813
PORI11	0	5.929825	0.687582
PORI8	0	5.859649	0.707168
GSPNG	0	7.315789	0.725248
PORI3	0	2.54386	0.742529

Biotope 3 - 4

Taxa	Biotope 3 Average	Biotope 4 Average	Cumulative Summary
CID	0.25	34.37037	0.429501
CERI	0.25	31.2716	0.517205
PARA	4	1.17284	0.599895
YSPNG	0.25	13.2963	0.666212
CNI4	2.5	0.37037	0.715019

Biotope 3 - 5

Taxa	Biotope 3 Average	Biotope 5 Average	Cumulative Summary
CNI8	0	32.9697	0.178927
GSPNG	0	59.16667	0.353131
MAD	0	15.69697	0.430893
CNI14	0	8.787879	0.480539
PARA	4	0.227273	0.528287
BOWL	0	8.651515	0.567195
CNI4	2.5	0.530303	0.596946
WSQUAT	0	6.863636	0.623889
HOLO1	2.75	0.030303	0.650052
RET	0	4.106061	0.672329
HOLO3	0	3.590909	0.694212

CERI	0.25	1.30303	0.715643
FAN1	0	4.121212	0.735199
CNI6	0	3.272727	0.75023

Biotope 3 - 6

Taxa	Biotope 3 Average	Biotope 6 Average	Cumulative Summary
URCH5	0.25	296.2188	0.617275
PARA	4	0.28125	0.684945
HOLO1	2.75	0.9375	0.724612
CNI4	2.5	0.375	0.754225

Biotope 3 - 8

Taxa	Biotope 3 Average	Biotope 8 Average	Cumulative Summary
URCH1	0	38.15556	0.365879
CNI1	0	7.977778	0.526431
PARA	4	0.177778	0.629684
URCH2	0	3.644444	0.681925
CNI4	2.5	0.533333	0.733187

Biotope 3 - 9

Taxa	Biotope 3 Average	Biotope 9 Average	Cumulative Summary
LOPH	0	73.3	0.495631
SCORA19	0	15.05	0.564269
STAR7	0	11.2	0.624263
LEIO	0	6.05	0.665853
PARA	4	0.05	0.706348
MAJ1	0	3.7	0.73035
HOLO1	2.75	0	0.753258

Biotope 3 - 11

Taxa	Biotope 3 Average	Biotope 11 Average	Cumulative Summary
PARA	4	0	0.17291
OPHI2	0.25	6.375	0.341075
CERI	0.25	4.625	0.474563
HOLO1	2.75	0	0.543418
CNI4	2.5	0	0.609583
CORALY2	0	1.375	0.654677
CALVE	1	0	0.695257
OPHI4	0	0.875	0.728024

Biotope 3 - 12

Taxa	Biotope 3 Average	Biotope 12 Average	Cumulative Summary
CNI14	0	26.38596	0.115685
OPHI4	0	135.2807	0.22099
SOLE	0	47.61404	0.325522
PEN2	0	28.78947	0.423333
EUPL2	0	25.35088	0.484129

YSPNG	0.25	18.4386	0.541405
CERI	0.25	3.45614	0.573601
OPHI2	0.25	6.22807	0.604417
ASC1	0	7.684211	0.63372
PARA	4	0.017544	0.661944
PORI11	0	5.929825	0.688224
PORI8	0	5.859649	0.707309
GSPNG	0	7.315789	0.724215
HOLO1	2.75	0.017544	0.74102

Biotope 4 - 5

Taxa	Biotope 4 Average	Biotope 5 Average	Cumulative Summary
CID	34.3704	1.651515	0.171345
GSPNG	0.33333	59.16667	0.31376
CNI8	0.01235	32.9697	0.444845
CERI	31.2716	1.30303	0.511411
MAD	0.54321	15.69697	0.57176
YSPNG	13.2963	1.772727	0.611872
HOLO3	6.82716	3.590909	0.650707
CNI14	0.06173	8.787879	0.686598
BOWL	0	8.651515	0.717348
WSQUAT	0	6.863636	0.738403

Biotope 4 - 6

Taxa	Biotope 4 Average	Biotope 6 Average	Cumulative Summary
URCH5	0	296.2188	0.490238
CID	34.3704	2.5625	0.678963
CERI	31.2716	0.5	0.736415

Biotope 4 - 8

Taxa	Biotope 4 Average	Biotope 8 Average	Cumulative Summary
CID	34.3704	2.688889	0.299349
URCH1	0.28395	38.15556	0.542616
CNI1	0.03704	7.977778	0.638068
CERI	31.2716	0.777778	0.719978

Biotope 4 - 9

Taxa	Biotope 4 Average	Biotope 9 Average	Cumulative Summary
LOPH	1.28395	73.3	0.362307
CID	34.3704	0.35	0.528319
CERI	31.2716	0	0.585816
SCORA19	0	15.05	0.64112
STAR7	0.02469	11.2	0.686729
YSPNG	13.2963	0	0.723099
LEIO	0	6.05	0.754047

Biotope 4 - 11

Taxa	Biotope 4 Average	Biotope 11 Average	Cumulative Summary
CID	34.3704	0	0.388179
CERI	31.2716	4.625	0.525901
OPHI2	0.02469	6.375	0.620035
YSPNG	13.2963	0.25	0.679222
HOLO3	6.82716	0	0.722058
CORALY2	0	1.375	0.745585

Biotope 4 - 12

Taxa	Biotope 4 Average	Biotope 12 Average	Cumulative Summary
CID	34.3704	1.403509	0.125072
OPHI4	0	135.2807	0.221798
SOLE	0.08642	47.61404	0.312755
CNI14	0.06173	26.38596	0.40097
PEN2	0	28.78947	0.480102
CERI	31.2716	3.45614	0.545739
YSPNG	13.2963	18.4386	0.608456
EUPL2	0	25.35088	0.658568
OPHI2	0.02469	6.22807	0.681813
ASC1	0	7.684211	0.705035
PORI11	0.1358	5.929825	0.725522
HOLO3	6.82716	0	0.745841

Biotope 5 - 6

Taxa	Biotope 5 Average	Biotope 6 Average	Cumulative Summary
URCH5	0.04545	296.2188	0.420248
GSPNG	59.1667	2.375	0.535817
CNI8	32.9697	1.65625	0.637789
MAD	15.697	5.96875	0.688887
BOWL	8.65152	3.5625	0.719276
CNI14	8.78788	0	0.747382

Biotope 5 - 8

Taxa	Biotope 5 Average	Biotope 8 Average	Cumulative Summary
URCH1	0	38.15556	0.166427
GSPNG	59.1667	0	0.317807
CNI8	32.9697	0	0.461469
MAD	15.697	0	0.526733
CNI1	0	7.977778	0.58537
CNI14	8.78788	0	0.624764
BOWL	8.65152	0	0.657879
WSQUAT	6.86364	0.088889	0.680729
URCH2	0	3.644444	0.700597
CID	1.65152	2.688889	0.72012
RET	4.10606	0	0.738361

Biotope 5 - 9

Taxa	Biotope 5 Average	Biotope 9 Average	Cumulative Summary
LOPH	1.74242	73.3	0.285298
GSPNG	59.1667	2.5	0.41189
CNI8	32.9697	1.9	0.511757
MAD	15.697	1.3	0.562494
SCORA19	0	15.05	0.609368
STAR7	3.57576	11.2	0.648152
CNI14	8.78788	0.55	0.676423
LEIO	3.4697	6.05	0.703591
BOWL	8.65152	0.25	0.729881
WSQUAT	6.86364	0.55	0.747835

Biotope 5 - 11

Taxa	Biotope 5 Average	Biotope 11 Average	Cumulative Summary
GSPNG	59.1667	0.625	0.173984
CNI8	32.9697	0.125	0.347922
MAD	15.697	0	0.424735
OPHI2	0.07576	6.375	0.483534
CNI14	8.78788	0.875	0.534248
CERI	1.30303	4.625	0.581212
BOWL	8.65152	0	0.619801
WSQUAT	6.86364	0	0.646425
RET	4.10606	0	0.668335
HOLO3	3.59091	0	0.689823
FAN1	4.12121	0	0.70914
CNI6	3.27273	0.125	0.724128
BSPNG	0.95455	1.25	0.738735
CORALY2	0.01515	1.375	0.752997

Biotope 5 - 12

Taxa	Biotope 5 Average	Biotope 12 Average	Cumulative Summary
GSPNG	59.1667	7.315789	0.106188
OPHI4	1.16667	135.2807	0.199387
SOLE	1.60606	47.61404	0.282495
CNI8	32.9697	1.508772	0.362457
PEN2	0.06061	28.78947	0.429879
CNI14	8.78788	26.38596	0.494447
EUPL2	0.13636	25.35088	0.538028
MAD	15.697	0	0.578699
YSPNG	1.77273	18.4386	0.616525
BOWL	8.65152	0.017544	0.637908
ASC1	1.74242	7.684211	0.658586
OPHI2	0.07576	6.22807	0.677475
CERI	1.30303	3.45614	0.695488

PORI11	0.01515	5.929825	0.712402
WSQUAT	6.86364	0.561404	0.72732
PORI8	0	5.859649	0.741671
FAN1	4.12121	1.824561	0.754677

Biotope 6 - 8

Taxa	Biotope 6 Average	Biotope 8 Average	Cumulative Summary
URCH5	296.219	0	0.52572
URCH1	0	38.15556	0.703687

Biotope 6 - 9

Taxa	Biotope 6 Average	Biotope 9 Average	Cumulative Summary
URCH5	296.219	0	0.411813
LOPH	0.28125	73.3	0.686043
SCORA19	0	15.05	0.728643

Biotope 6 - 11

Taxa	Biotope 6 Average	Biotope 11 Average	Cumulative Summary
URCH5	296.219	0	0.601554
OPHI2	0.03125	6.375	0.67156
CERI	0.5	4.625	0.723042
MAD	5.96875	0	0.749663

Biotope 6 - 12

Taxa	Biotope 6 Average	Biotope 12 Average	Cumulative Summary
URCH5	296.219	2.368421	0.346731
OPHI4	0	135.2807	0.43023
SOLE	0	47.61404	0.503515
CNI14	0	26.38596	0.571171
PEN2	0	28.78947	0.632615
EUPL2	0	25.35088	0.67242
YSPNG	0.59375	18.4386	0.707932
ASC1	0.5625	7.684211	0.725957
OPHI2	0.03125	6.22807	0.743561

Biotope 8 - 9

Taxa	Biotope 8 Average	Biotope 9 Average	Cumulative Summary
LOPH	0	73.3	0.403241
URCH1	38.1556	0	0.565232
SCORA19	0	15.05	0.624948
CNI1	7.97778	0	0.679264
STAR7	0	11.2	0.729195

Biotope 8 - 11

Taxa	Biotope 8 Average	Biotope 11 Average	Cumulative Summary
URCH1	38.1556	0	0.343617
CNI1	7.97778	0	0.492364
OPHI2	0	6.375	0.605148

CERI	0.77778	4.625	0.686415
URCH2	3.64444	0	0.735092

Biotope 8 - 12

Taxa	Biotope 8 Average	Biotope 12 Average	Cumulative Summary
URCH1	38.1556	0	0.12555
OPHI4	0	135.2807	0.224533
CNI14	0	26.38596	0.320674
SOLE	0	47.61404	0.415984
PEN2	0	28.78947	0.500792
EUPL2	0	25.35088	0.554041
YSPNG	0	18.4386	0.604111
CNI1	7.97778	0.052632	0.644285
OPHI2	0	6.22807	0.66957
ASC1	0	7.684211	0.694587
CERI	0.77778	3.45614	0.718754
PORI11	0	5.929825	0.74088

Biotope 9 - 11

Taxa	Biotope 9 Average	Biotope 11 Average	Cumulative Summary
LOPH	73.3	0	0.476078
SCORA19	15.05	0	0.543043
STAR7	11.2	0	0.600954
OPHI2	0	6.375	0.652872
LEIO	6.05	0	0.692879
CERI	0	4.625	0.732013

Biotope 9 - 12

Taxa	Biotope 9 Average	Biotope 12 Average	Cumulative Summary
LOPH	73.3	0	0.220024
OPHI4	0.15	135.2807	0.309165
SOLE	0.35	47.61404	0.389378
CNI14	0.55	26.38596	0.456486
PEN2	0	28.78947	0.521554
EUPL2	0	25.35088	0.563678
YSPNG	0	18.4386	0.601665
SCORA19	15.05	0	0.638916
STAR7	11.2	0.105263	0.667772
LEIO	6.05	0.649123	0.686625
ASC1	0	7.684211	0.705367
OPHI2	0	6.22807	0.723261
PORI11	0	5.929825	0.739445

Biotope 11 - 12

Taxa	Biotope 11 Average	Biotope 12 Average	Cumulative Summary
OPHI4	0.875	135.2807	0.11465

CNI14	0.875	26.38596	0.229153
SOLE	0.125	47.61404	0.340384
PEN2	0	28.78947	0.443266
EUPL2	0.25	25.35088	0.50624
YSPNG	0.25	18.4386	0.566737
OPHI2	6.375	6.22807	0.622064
ASC1	0	7.684211	0.652764
CERI	4.625	3.45614	0.683156
PORI11	0	5.929825	0.710595
PORI8	0	5.859649	0.730846
GSPNG	0.625	7.315789	0.749904

7.3 Results from indVal analysis per biotope indicating the most representative species in each community

The most representative species in each community were identified using the indicator value index (IndVal) where values of IndVal range between from 0 to 100% (Dufrière & Legendre, 1997). A value of 100% for a particular species would indicate that it is encountered exclusively in each group and at every station. (Dufrière & Legendre, 1997). Biotopes seven and ten were manually assessed as they are single species biotopes and SIMPER requires a minimum of two terminal nodes present in a group to successfully run.

Biotope 1				
	IndVal Group	Indval	P-value	Frequency
HOLO4/ Holothuroidea Species 4	1 (Biotope 1)	0.949825	1.00E-04	13
CNI12/ Anthozoa Species 12	1 (Biotope 1)	0.333333	0.0169	1
CNI5/ Anthozoa Species 5	1 (Biotope 1)	0.291601	0.0364	19
CNI2	1 (Biotope 1)	0.19177*	0.1318	12
BUCC	1 (Biotope 1)	0.113346*	0.3094	25
Biotope 2				
	IndVal Group	Indval	P-value	Frequency
OPHI3/ Ophiuroidea Species 3	2 (Biotope 2)	0.92876	2.00E-04	6
OPHI1/ Ophiuroidea Species 1	2 (Biotope 2)	0.752791	7.00E-04	17
POMP/ <i>Liponema brevicorne</i>	2 (Biotope 2)	0.425373	0.015	5
EPIZOA/ <i>Epizoanthus paguriphilus</i>	2 (Biotope 2)	0.345462	0.0262	10
Biotope 3				
	IndVal Group	Indval	P-value	Frequency
PARA/ <i>Parastichopus</i> sp.	3 (Biotope 3)	0.622405	0.0024	71
CNI4/	3 (Biotope 3)	0.268247*	0.0646	44
CALVE	3 (Biotope 3)	0.235756*	0.0836	68
HOLO1	3 (Biotope 3)	0.168056*	0.149	16
CNI7	3 (Biotope 3)	0.129787*	0.2076	10
STAR4	3 (Biotope 3)	0.077925*	0.4033	19
Biotope 4				
	IndVal Group	Indval	P-value	Frequency
CID/ <i>Cidaris cidaris</i>	4 (Biotope 4)	0.779195	1.00E-04	170
STYL	4 (Biotope 4)	0.118025*	0.1926	11
URCH4	4 (Biotope 4)	0.138608*	0.2029	16
CERI	4 (Biotope 4)	0.233346*	0.2031	117
CUP	4 (Biotope 4)	0.049383*	0.2168	4
SQUAT	4 (Biotope 4)	0.150636*	0.2219	53

SPEN1	4 (Biotope 4)	0.049383*	0.2414	4
SPNG1	4 (Biotope 4)	0.037037*	0.2642	3
STAR3	4 (Biotope 4)	0.024691*	0.4283	2
CARO	4 (Biotope 4)	0.054094*	0.5145	20
STAR2	4 (Biotope 4)	0.016403*	0.7082	5
STAR5	4 (Biotope 4)	0.012346*	1	1

Biotope 5

	IndVal Group	Indval	P-value	Frequency
CNI8/ Anthozoa Species 8	5 (Biotope 5)	0.811366	2.00E-04	119
GSPNG/ Demospongiae	5 (Biotope 5)	0.694206	0.0039	110
WSQUAT/ Galatheaidea	5 (Biotope 5)	0.565245	0.0086	73
MAD/ <i>Madrepora oculata</i>	5 (Biotope 5)	0.428936	0.016	65
CNI6/ Anthozoa Species 6	5 (Biotope 5)	0.414821	0.0201	40
BOWL/ Phakellia Species 1	5 (Biotope 5)	0.378078	0.0205	45
RET/ Reteporella	5 (Biotope 5)	0.330379	0.0452	53
FAN1	5 (Biotope 5)	0.298272*	0.0565	69
STICHO	5 (Biotope 5)	0.249*	0.0695	31
ANTHO	5 (Biotope 5)	0.227273*	0.0999	15
VNUS	5 (Biotope 5)	0.19448*	0.1205	33
STAR1	5 (Biotope 5)	0.173001*	0.165	48
URCH7	5 (Biotope 5)	0.106061*	0.193	7
SCORA13	5 (Biotope 5)	0.106061*	0.1941	7
ACNT2	5 (Biotope 5)	0.060606*	0.1978	4
PORI23	5 (Biotope 5)	0.121212*	0.211	8
EUPL	5 (Biotope 5)	0.145862*	0.2126	44
SCORA18	5 (Biotope 5)	0.060606*	0.2171	4
SCORA15	5 (Biotope 5)	0.060606*	0.2263	4
UNK6	5 (Biotope 5)	0.100487*	0.2324	9
BATHY2	5 (Biotope 5)	0.07208*	0.2378	8
HYMN	5 (Biotope 5)	0.125369*	0.2634	20
CNI17	5 (Biotope 5)	0.030303*	0.2648	2
PORI1	5 (Biotope 5)	0.101701*	0.2671	16
HYDRO2	5 (Biotope 5)	0.087977*	0.2681	12
SCORA21	5 (Biotope 5)	0.030303*	0.2937	2
CNI19	5 (Biotope 5)	0.030303*	0.3004	2
BRYOZ1	5 (Biotope 5)	0.110674*	0.3069	27
URCH8	5 (Biotope 5)	0.030303*	0.3125	2
SCORA16	5 (Biotope 5)	0.051486*	0.3143	6
BATHY3	5 (Biotope 5)	0.058651*	0.3206	7
HOLO3	5 (Biotope 5)	0.111117*	0.3252	43
SCORA4	5 (Biotope 5)	0.030303*	0.3298	2
OCTOP	5 (Biotope 5)	0.048876*	0.3405	6
ISI1	5 (Biotope 5)	0.092979*	0.3643	20

SABEL	5 (Biotope 5)	0.028991*	0.3891	3
STAR10	5 (Biotope 5)	0.032437*	0.4086	6
SPHERI1	5 (Biotope 5)	0.035387*	0.4118	5
CORALY1	5 (Biotope 5)	0.021453*	0.4688	3
CNI11	5 (Biotope 5)	0.019192*	0.5227	3
CNI13	5 (Biotope 5)	0.037699*	0.5688	13
FSTAR2	5 (Biotope 5)	0.051925*	0.5854	20
PARA2	5 (Biotope 5)	0.031519*	0.6001	10
URCH10	5 (Biotope 5)	0.015152*	0.7369	1
HOLO6	5 (Biotope 5)	0.015152*	0.7413	1
CORA1	5 (Biotope 5)	0.015152*	0.7419	1
CNI18	5 (Biotope 5)	0.015152*	0.7425	1
HYDRO1	5 (Biotope 5)	0.015152*	0.7443	1
SCORA14	5 (Biotope 5)	0.015152*	0.7444	1
DRIF	5 (Biotope 5)	0.015152*	0.7448	1
UKN2	5 (Biotope 5)	0.015152*	0.7469	1
CORALY	5 (Biotope 5)	0.015152*	0.7475	1
URCH9	5 (Biotope 5)	0.015152*	0.7493	1
UNK5	5 (Biotope 5)	0.015152*	0.7499	1
CUP2	5 (Biotope 5)	0.015152*	0.7543	1
OSPNG	5 (Biotope 5)	0.010766*	0.7987	2

Biotope 6

	IndVal Group	Indval	P-value	Frequency
CYCLO	6 (Biotope 6)	0.09375*	0.1265	3
PORI2	6 (Biotope 6)	0.129343*	0.1651	15
UMBEL	6 (Biotope 6)	0.03125*	0.218	1
CNI3	6 (Biotope 6)	0.01741*	0.7075	5

Biotope 8

	IndVal Group	Indval	P-value	Frequency
URCH1/ Echinoidea Species 1	7 (Biotope 8)	0.926439	1.00E-04	49
CNI1/ Anthozoa Species 1	7 (Biotope 8)	0.608238	0.0041	36
URCH2/ Echinoidea Species 2	7 (Biotope 8)	0.497625	0.0059	26
PAGU	7 (Biotope 8)	0.269334*	0.059	57
HOLO2	7 (Biotope 8)	0.047199*	0.2954	5
TCERI	7 (Biotope 8)	0.022222*	0.3666	1
PEN1	7 (Biotope 8)	0.026068*	0.4961	5
NYMPH1	7 (Biotope 8)	0.013213*	0.6752	2

Biotope 9

	IndVal Group	Indval	P-value	Frequency
LOPH/ <i>Desmophyllum pertusum</i>	8 (Biotope 9)	0.956824	1.00E-04	57
STAR7/ Asteroidea	8 (Biotope 9)	0.594876	0.0065	54
CALLO/ Callogorgia Species 1	8 (Biotope 9)	0.445386	0.0109	31

CHAC/ Chaceon Species 1	8 (Biotope 9)	0.342586	0.024	28
SCORA2/ <i>Flabellum alabastrum</i>	8 (Biotope 9)	0.372204	0.0257	32
LEIO/ Leopathes Species	8 (Biotope 9)	0.354793	0.0271	59
MAJ1/ Decapoda	8 (Biotope 9)	0.350271	0.0292	45
SCORA19/ Flebellidae	8 (Biotope 9)	0.3	0.0374	6
CRAB2	8 (Biotope 9)	0.225913*	0.0686	8
SCORA20	8 (Biotope 9)	0.190385*	0.0964	5
BRIS4	8 (Biotope 9)	0.1*	0.1016	2
SCORA1	8 (Biotope 9)	0.201577*	0.1055	27
STAR15	8 (Biotope 9)	0.05*	0.1173	1
SCORA6	8 (Biotope 9)	0.206963*	0.1203	18
CRAB1	8 (Biotope 9)	0.143983*	0.1362	10
SCORA17	8 (Biotope 9)	0.164413*	0.1389	7
PORI24	8 (Biotope 9)	0.083193*	0.1637	4
SCORA12	8 (Biotope 9)	0.042537*	0.1723	2
CALLO2	8 (Biotope 9)	0.038372*	0.201	2
GORGO	8 (Biotope 9)	0.130952*	0.2366	14
SCORA9	8 (Biotope 9)	0.128722*	0.2533	25
SCORA10	8 (Biotope 9)	0.115764*	0.3	28
YSPNG2	8 (Biotope 9)	0.084629*	0.3442	18
YSPNG3	8 (Biotope 9)	0.029381*	0.3507	3
URCH6	8 (Biotope 9)	0.048529*	0.3737	7
CNI10	8 (Biotope 9)	0.039658*	0.5393	10

Biotope 11

	IndVal Group	Indval	P-value	Frequency
CORALY2	9 (Biotope 11)	0.461976	0.0082	28
OPHI2/ Ophiuroidea Species 2	9 (Biotope 11)	0.36822	0.0315	35
UKN1	9 (Biotope 11)	0.216179*	0.1022	13

Biotope 12

	IndVal Group	Indval	P-value	Frequency
CNI14/ Anthozoa Species 4	10 (Biotope 12)	0.719737	1.00E-04	104
PEN2/ Parantipathes	10 (Biotope 12)	0.857843	2.00E-04	51
EUPL2/ <i>Asconema foliatum</i>	10 (Biotope 12)	0.846744	0.0011	55
PORI11/ Porifera Species 6	10 (Biotope 12)	0.633008	0.0029	40
ASC1/ Ascidiacea Species 1	10 (Biotope 12)	0.607308	0.003	66
SOLE/ <i>Solenosmilia variabilis</i>	10 (Biotope 12)	0.6712	0.0039	63
OPHI4/ Ophiuroidea Species 4	10 (Biotope 12)	0.690567	0.0057	58
BRIS1/ Brisingida Species 1	10 (Biotope 12)	0.548258	0.006	40
PORI10/ Porifera Species 5	10 (Biotope 12)	0.521391	0.0078	52
PENTA/ Pentametrocrinus	10 (Biotope 12)	0.457448	0.0079	30
CNI9/ Anthozoa Species 9	10 (Biotope 12)	0.44076	0.0113	32
YSPNG/ Demospongiae	10 (Biotope 12)	0.448746	0.0208	127
FSTAR1/ Crinoidea Species 1	10 (Biotope 12)	0.373628	0.0274	60

VNUS2/ Actinoscyphia	10 (Biotope 12)	0.305795	0.0281	27
PORI12/ Porifera Species 12	10 (Biotope 12)	0.359398	0.0303	25
PORI3/ Porifera Species 3	10 (Biotope 12)	0.36152	0.0304	30
SHRMP/ Shrimp Species	10 (Biotope 12)	0.303911	0.0409	36
YSNG3/ <i>Aplysilla sulfurea</i>	10 (Biotope 12)	0.315789	0.0452	18
FSTAR4/ Crinoidea Species 4	10 (Biotope 12)	0.280702	0.0516	16
PORI8	10 (Biotope 12)	0.285769*	0.0556	27
YEUPL2	10 (Biotope 12)	0.263158*	0.0627	15
UNK3	10 (Biotope 12)	0.263158*	0.0643	15
PEN3	10 (Biotope 12)	0.244128*	0.0706	27
BSPNG	10 (Biotope 12)	0.249634*	0.0973	70
PURP	10 (Biotope 12)	0.210526*	0.1063	12
BATHY	10 (Biotope 12)	0.19805*	0.1066	29
PORI9	10 (Biotope 12)	0.201248*	0.1161	27
UKN3	10 (Biotope 12)	0.173517*	0.1167	11
SCORA7	10 (Biotope 12)	0.105263*	0.1196	6
BRIS3	10 (Biotope 12)	0.152819*	0.1255	11
PORI13	10 (Biotope 12)	0.175439*	0.137	10
PORI4	10 (Biotope 12)	0.17085*	0.1462	14
SCORA8	10 (Biotope 12)	0.166088*	0.1492	14
CNI16	10 (Biotope 12)	0.087719*	0.1574	5
OPHI5	10 (Biotope 12)	0.105263*	0.1602	6
BRIS2	10 (Biotope 12)	0.052632*	0.1615	3
PORI6	10 (Biotope 12)	0.052632*	0.1718	3
UNK4	10 (Biotope 12)	0.105263*	0.1721	6
YSNP	10 (Biotope 12)	0.052632*	0.1734	3
FSTAR7	10 (Biotope 12)	0.052632*	0.1819	3
ISI2	10 (Biotope 12)	0.153971*	0.1852	34
PORI20	10 (Biotope 12)	0.070175*	0.1874	4
PORI14	10 (Biotope 12)	0.122807*	0.1883	7
OCTO	10 (Biotope 12)	0.052632*	0.1917	3
PEN4	10 (Biotope 12)	0.095007*	0.1936	7
PYCNO	10 (Biotope 12)	0.122807*	0.199	7
YEUPL	10 (Biotope 12)	0.070175*	0.2016	4
STAR8	10 (Biotope 12)	0.092018*	0.2022	7
PORI15	10 (Biotope 12)	0.035088*	0.2191	2
PORI16	10 (Biotope 12)	0.035088*	0.2313	2
PORI7	10 (Biotope 12)	0.035088*	0.2313	2
FSTAR3	10 (Biotope 12)	0.081734*	0.246	8
PORI19	10 (Biotope 12)	0.035088*	0.252	2
STAR12	10 (Biotope 12)	0.035088*	0.2536	2
SCORA5	10 (Biotope 12)	0.035088*	0.2563	2
PORI5	10 (Biotope 12)	0.05984*	0.257	5

ECHI	10 (Biotope 12)	0.11265*	0.2688	33
STAR14	10 (Biotope 12)	0.039118*	0.3315	5
SCORA3	10 (Biotope 12)	0.090246*	0.3368	14
STAR13	10 (Biotope 12)	0.027245*	0.3477	3
SCORA11	10 (Biotope 12)	0.026991*	0.3704	4
CNI15	10 (Biotope 12)	0.034668*	0.3951	6
PORI21	10 (Biotope 12)	0.017544*	0.5357	1
STAR11	10 (Biotope 12)	0.017544*	0.536	1
PORI18	10 (Biotope 12)	0.017544*	0.5366	1
UNK1	10 (Biotope 12)	0.017544*	0.5373	1
STAR9	10 (Biotope 12)	0.017544*	0.5385	1
PORI17	10 (Biotope 12)	0.017544*	0.5391	1
HOLO5	10 (Biotope 12)	0.017544*	0.5396	1
HOLO15	10 (Biotope 12)	0.017544*	0.5401	1
PYGNO	10 (Biotope 12)	0.017544*	0.5419	1
PORI22	10 (Biotope 12)	0.017544*	0.5459	1
PORA	10 (Biotope 12)	0.028279*	0.7118	12
STAR6	10 (Biotope 12)	0.006833*	1	3

*IndVal value that was non-significant (P -value greater than 0.05)

7.4 Fusion levels from the dendrogram of \log_{x+1} and Hellinger with Bray-Curtis UPGMA clustering

Fusion levels are used to depict dissimilarity values where fusion between two branches of a dendrogram occur. Subsequent plotting of these fusion levels helps to define cutting levels in the dendrogram (Borcard et al., 2011).

